

Studies on the factors associated with the cell adaptation of the rabies vaccine strain

HEP-Flury

日本語: 狂犬病ウイルス HEP-Flury 株の細胞馴化関連因子に関する研究

Joint Graduate School of Veterinary Medicine

Yamaguchi University

Michiko HARADA

September 2024

Index

1. General introduction	5
1.1 Rabies history	5
1.2 Virus structure	6
1.3 Pathogenesis	8
1.4 Treatment and prevention	9
1.5 Human rabies vaccine	10
2. Chapter1: Construction of Vero cell-adapted rabies vaccine strain by five amino acid substitutions in HEP-Flury strain.	13
2.1 Abstract	13
2.2 Introduction	15
2.3 Materials and Methods	19
2.3.1 Cells	19
2.3.2 Viruses	19
2.3.3 Adaptation of HEP-Flury strain to propagation in the Vero cell line	20
2.3.4 Virus titration	20
2.3.5 Comparison of viral growth	21
2.3.6 Observation of plaques	21
2.3.7 Inoculation of rabbits with rabies vaccines	22
2.3.8 Challenge experiment in mice with each HEP	23
2.3.9 Reverse transcription-polymerase chain reaction (RT-PCR)	24
2.3.10 Sequence analysis	25
2.3.11 Rapid fluorescent focus inhibition test (RFFIT)	25
2.3.12 Immunoblot analysis	26
2.3.13 Construction of plasmids for reverse genetics	27
2.3.14 Rescue of recombinant viruses	28
2.3.15 Comparison of efficiency of cell infection	29
2.3.16 Flow cytometric analysis	30
2.3.17 Production of pseudotyped vesicular stomatitis virus (VSVp)	30
2.3.18 Titration of VSVp	31
2.3.19 Quantification of infection with VSVp	32
2.3.20 Statistical analysis	32
2.4 Results	34
2.4.1 Adaptation of HEP-Flury to Vero cells	34
2.4.2 Comparison of viral growth of HEP and adapted HEPs in Vero cells	35

2.4.3	Comparison of expression of viral proteins by HEP and the adapted HEPs	36
2.4.4	Comparison of antigenicity between HEP and Vero-adapted HEPs.....	36
2.4.5	Comparison of pathogenicity between HEP and adapted HEPs	37
2.4.6	Comparison of VNA activity using sera from mice infected with HEP or adapted HEPs	38
2.4.7	Comparison of the viral genomes among HEP, HEP-10V, and HEP-30V	38
2.4.8	Comparison of viral growth in Vero cells of recombinant HEP and HEP-10V viruses	39
2.4.9	Comparison of virus entry in Vero cells by recombinant viruses	40
2.4.10	Comparison of cell surface accumulation of viral proteins by recombinant HEP-Flury strains	41
2.4.11	Comparison of viral growth among recombinant HEP-10V with each mutation in HEP-30V	42
2.4.12	Comparison of viral entry using VSVp pseudotyped with the G protein of HEP-30V	43
2.4.13	Comparison of viral growth among recombinant viruses with five mutations	44
2.5	Discussion	45
2.6	Figure legends	52
2.7	Figure and tables.....	60
2.8	Supplementary Table	68
3.	Chapter 2: Single amino acid substitution in the matrix protein of rabies virus is associated with neurovirulence in mice.....	78
3.1	Abstract	78
3.2	Introduction	79
3.3	Materials and Methods	82
3.3.1	Cells and Viruses	82
3.3.2	Reverse transcription-polymerase chain reaction (RT-PCR).....	82
3.3.3	Constructing and rescuing recombinant RABVs.....	83
3.3.4	Virus titration	84
3.3.5	Comparing viral growth	85
3.3.6	Animal experiments.....	85
3.3.7	Statistical analysis.....	86
3.4	Results	87
3.4.1	Comparison of viral growth between original and recombinant HEP	87
3.4.2	Comparing viral growth of limiting dilution viruses	88
3.4.3	Comparison of viral growth of recombinant HEP-M(D80N).....	88

3.4.4 Pathogenicity of recombinant HEP-M(D80N).....	89
3.5 Discussion	91
3.6 Figure legends.....	94
3.7 Figure and tables.....	97
3.8 Supplemental figure and table.....	99
4. General conclusion	105
5. Acknowledgements.....	107
6. Reference.....	109

1. General introduction

1.1 Rabies history

Rabies is a fatal zoonotic disease that causes encephalitis in almost all species of mammals. Rabies virus can be detected in the brain and saliva of infected animals, most commonly dogs, and transmitted by bite¹. Dog-mediated rabies has been reported throughout world, especially in Asia and Africa¹. The number of human deaths by rabies is estimated at 59,000 annually², and more than 99% of human rabies is transmitted by dogs. In Asia, an estimated 35,172 people die each year from dog-transmitted rabies, and 21,476 people died each year in Africa². The number of countries that have eliminated rabies, including Japan, is small, and these rabies-free countries are still at risk of imported cases³. Recently, a case of imported human rabies was reported in Japan in 2020⁴.

Rabies has affected humans for more than 4000 years⁵. In 1885, Louis Pasteur developed the human rabies vaccine from rabbit spinal cord emulsion, and the vaccine could prevent the onset of rabies in human patients⁶. The rabies vaccines have led to a reduction in the incidence of rabies worldwide and the successful elimination in Japan.

A plan called “Zero by 30” was launched in 2015 with the goal of achieving zero human deaths from dog-mediated rabies by 2030^{5,7}. This plan is supported by the “United

Against Rabies” initiative, formed by the World Health Organization (WHO), the World Organization for Animal Health (OIE), the Food and Agriculture Organization of the United Nations (FAO), and the Global Alliance for Rabies Control (GARC). This plan has focused on three objectives: reducing the risk of human rabies, providing guidance and data, and leveraging multi-stakeholder engagement^{5,7}. The tasks to reduce the risk of human rabies include administering human rabies vaccine and immunoglobulin against rabies virus, and organizing canine vaccination campaigns; providing guidance and sharing data to improve the education and information that lead to reduced exposure to rabies; and leveraging multi-stakeholder engagement to eliminate rabies in individual countries and regions. These activities are being carried out around the world to eliminate human rabies from dogs.

1.2 Virus structure

Rabies is caused by infection with rabies virus (RABV) which is non-segmented, single negative-stranded RNA virus belonging to the order *Mononegavirales*, the family *Rhabdoviridae* and genus *Lyssavirus*⁸. The RABV virion is bullet-shaped and has an approximately 12 kb non-segmented RNA genome of negative polarity that encodes five viral proteins including nucleoprotein (N protein), phosphoprotein (P protein), matrix

protein (M protein), glycoprotein (G protein) and large RNA-dependent RNA polymerase protein (L protein)^{1,8}. RABV replicates in the cytoplasm of the host cell. First, RABV enters the host cell by endocytosis mediated by a binding receptor, followed by membrane fusion at acidic pH and subsequent release of the viral ribonucleoprotein (RNP) into the cytoplasm. Next, six transcripts are produced, including the full-length positive-strand RNA and five mRNAs encoding N, P, M, G and L proteins, followed by replication of viral genome. Finally, RABV is transported to the cell membrane where assembly and budding occur⁸⁻¹⁰.

The N protein forms an RNP complex with the P and the L proteins, which then stimulates RABV mRNA transcription and full-length genomic RNA replication. The P protein has multiple functions such as regulating replication and transcription, facilitating the axonal transport, and inhibiting interferon (IFN) production. The M protein induces assembly and budding of virus. The G protein is associated with cell binding receptor, antigenicity and pathogenicity. The L protein stimulates genome replication, transcription with the P protein, and escape from host the innate immunity^{9,11-13}.

1.3 Pathogenesis

The RABV has two types of strains: the street strains and fixed strains. The street strains are highly virulent against mammals and when animals are inoculated intramuscularly with the street strain, clinical signs appear, leading to death. On the other hand, the fixed strains are attenuated, and the animals inoculated with fixed strain by intramuscular route, have limited onset of the disease. By transmission from the saliva of the infected animal by bite, RABV enters the body through the wound and infects peripheral nerves before spreading by retrograde axonal transport to the central nervous system (CNS)¹⁴. The first specific clinical symptoms are the pain at the site of the bite, after that show fever, back pain, confusion and so on. The pathogenesis depends on the virus reaching the CNS, where replication and neuronal network-dependent spread cause severe neurological symptoms, including agitation, hallucinations, seizures, convulsions, hydrophobia, aerophobia, and paralysis, preceding a fatal outcome^{4,14}. The incubation period of most cases is one to three months depending on the location of the bite, if the bite site is close to the brain such as in the arm, shoulder or neck, the onset may be faster than one month^{1,4}. On the other hand, in a small percentage of cases, the onset may take more than a year, in an exceptional case 8 years^{15,16}. However, despite of differences in the incubation period, once the disease appears, all patients die.

1.4 Treatment and prevention

The only known treatment for rabies is the Milwaukee protocol, but recovery rates by application of this protocol are low¹⁷⁻¹⁹. Thus, an effective treatment after the disease onset has not yet been established. However, vaccination before or after exposure and treatment of immunoglobulin are effective in preventing the onset of rabies^{1,7}. There are two types of rabies vaccination protocols, pre-exposure prophylaxis (PrEP) and post-exposure prophylaxis (PEP)¹. PrEP is recommended for people who are at high risk of exposure to rabies virus or bat lyssavirus because of their occupation, travel or residence in an endemic area with limited access to timely or adequate PEP. The vaccination schedule, recommended by the WHO as PrEP, is two doses (days 0 and 7) by intradermal or intramuscular injection¹, while in Japan it is recommended three times (days 0, 7, and 21 or 28) also by intradermal or intramuscular route. Exposure in the area where rabies is present is classified into three categories. Category I is only touching, feeding animals and getting licked on intact skin, it constitutes no exposure and it is not necessary to inoculate the PEP. Category II is bites and/or scratches without bleeding, and it requires the PEP. Category III is a single or multiple transdermal bites or scratches, contamination of mucous membranes with saliva from licks, licks on wound, exposure by direct contact with bat. In Category III, it is necessary to inoculate both PEP and immunoglobulin¹. The

vaccination schedule and protocol recommended by the WHO as PEP, is three or four doses (days 0, 3, and 7 / days 0, 7, and 21 / days 0, 3, 7, and 14) by intradermal or intramuscular injection¹, while in Japan five doses (days 0, 3, 7, 14 and 28) intradermal or intramuscular injections are recommended.

The human rabies vaccine has several varieties such as purified chicken embryo vaccine, purified Vero cell rabies vaccine, human diploid cell vaccine, duck embryo vaccine and neural tissue vaccines⁶. Neural tissue vaccine is not recommended by the WHO because they might induce side-effect such as acute disseminated encephalomyelitis (ADEM) when the neuronal-derived vaccine is inoculated into humans^{1,6}. In Japan, the chicken embryo vaccine has been licensed, with “Rabipur (GSK, Biologicals, Wavre, Belgium)” as the main vaccine.

1.5 Human rabies vaccine

The rabies viruses were serially passaged intracerebrally from rabbit to rabbit; these passaged strains were shown to have constant characteristics such as incubation period, symptoms, and titer in the brain as opposed to the street strain. They are known as “fixed strains” and were used for rabies vaccine development. The first successful prevention of rabies was in 1885. In this case, Dr. Pasteur produced an emulsion from the spinal cord

of a rabbit infected with the rabies virus passaged 20–25 times in rabbit brain and air-dried it for 14 days to prepare rabies vaccine. The boy who was bitten by a rabid dog was inoculated with this vaccine at 60 hours after exposure^{6,20}. To inactivate the rabies virus for its use as a rabies vaccine, Drs. Fermi and Semple treated sheep or goat brain tissues with phenol⁶. Since the vaccines produced by Drs. Pasteur, Fermi, and Semple were originated from nervous tissue, including myelin, these vaccines sometimes caused encephalitis and ADEM after vaccination. In the 1940s, these vaccine-induced allergic encephalomyelitis and CNS demyelinating lesions became problem²¹. Dr. Fuenzalida produced a rabies vaccine with 1% homogenized suckling mouse brain emulsion, but this vaccine also had similar severe adverse reactions²².

Dr. Goodpasture infected chicken embryos with fowl-pox virus or herpes simplex virus and succeeded in adapting the embryonated eggs, creating a new tool for virology and vaccine studies²³. As a result of this study, the Flury strain of rabies virus, isolated from a girl that developed rabies, was successfully adapted to 1-day-old chicks in 1940²⁴. Subsequently, the Flury strain was passaged 40–50 times in chicken eggs to generate the low-egg-passage Flury strain (LEP-Flury)^{6,25,26}. The original Flury strain has also been passaged in eggs 180 times or more to generate the high-egg-passage Flury strain (HEP-Flury)^{6,25–27}. LEP-Flury has pathogenicity in adult mice, while HEP-Flury is lethal only

in suckling mice, and not in adult mice^{26,28,29}. After this attenuated HEP-Flury strain was generated by continuous passaging, it was used to produce the purified chick embryo cell rabies vaccine (PCECV) in 1972, which has been manufactured in Japan since 1980^{6,25,30}. Another PCECV developed from the LEP-Flury strain is used in Europe and the USA⁶.

In 1962, the Vero cell line was established from African green monkey kidney cells and the polio vaccine was produced in this cell line in the late 1970s. Subsequently, the Pasteur viral strain, PV strain, was continuously passaged in Vero cells and the purified Vero cell rabies vaccine (PVRV) was generated in the early 1980s⁶. PVRV is widely used worldwide.

Rabies viruses were continuously passaged into animals or culture cell lines, and as the result of adaptation to the animals or cell lines, safe and cost-effective vaccines have been produced.

2. Chapter1: Construction of Vero cell-adapted rabies vaccine strain by five amino acid substitutions in HEP-Flury strain.

2.1 Abstract

Rabies virus (RABV) causes fatal neurological disease. Pre-exposure prophylaxis (PrEP) and post-exposure prophylaxis (PEP) using inactivated-virus vaccines are the most effective measures to prevent rabies. In Japan, HEP-Flury, the viral strain, used as a human rabies vaccine, has historically been propagated in primary fibroblast cells derived from chicken embryos. In the present study, to reduce the cost and labor of vaccine production, we sought to adapt the original HEP-Flury (HEP) to Vero cells. HEP was repeatedly passaged in Vero cells to generate ten- (HEP-10V) and thirty-passaged (HEP-30V) strains. Both HEP-10V and HEP-30V grew significantly better than HEP in Vero cells, with virulence and antigenicity similar to HEP. Comparison of the complete genomes with HEP revealed three non-synonymous mutations in HEP-10V and four additional non-synonymous mutations in HEP-30V. Experiments using 18 recombinant HEP strains constructed by reverse genetics and vesicular stomatitis virus pseudotyped with RABV glycoproteins indicated that the substitution P(L115H) in the phosphoprotein and G(S15R) in the glycoprotein improved viral propagation in HEP-10V, while in HEP-30V, G(V164E), G(L183P), and G(A286V) in the glycoprotein enhanced entry into Vero

cells. The obtained recombinant RABV strain, rHEP-PG4 strain, with these five substitutions, is a strong candidate for production of human rabies vaccine.

2.2 Introduction

Rabies is a lethal zoonotic disease that induces encephalitis in almost all species of mammals; the disease has been reported around the world, and is especially prevalent in Asia and Africa¹. Globally, the annual number of human deaths is estimated to be 59,000², and more than 99% of human rabies cases are transmitted by dogs⁸. The World Health Organization (WHO) is promoting “the global strategic plan to end human deaths from dog-mediated rabies by 2030: Zero by 30”⁵. Rabies vaccine for dogs have been recommended around the world^{31,32}, and the implementation of vaccine programs in each region has contributed to a reduction in the frequency of dog rabies, in turn resulting in a decrease in the number of human rabies cases¹.

The rabies virus (RABV) is a non-segmented, single stranded, negative-sense RNA virus that belongs to the order Mononegavirales, family *Rhabdoviridae*, subfamily *Alpharhabdovirinae*, genus *Lyssavirus*³³. The virus encodes 5 proteins, including the nucleoprotein (N protein), phosphoprotein (P protein), matrix (M) protein, glycoprotein (G protein) and a large RNA-dependent RNA polymerase (L protein)^{1,8,9,11–13}. The N protein forms a ribonucleoprotein (RNP) complex with the P and L proteins; the resulting complex promotes mRNA production as well as full-length genomic RNA replication^{9,13}. The P protein has multiple functions, including the regulation of replication and

transcription, facilitation of axonal transport, and inhibition of interferon (IFN) production by the host^{12,13,34}. The M protein induces the assembly and budding of novel viral particles¹³. The G protein is associated with binding to the cell receptor, induction of virus-neutralization antibodies (VNAs), and pathogenicity in humans and animals^{8-11,13}. The L protein, in combination with the P protein, is involved in the replication and transcription of the viral genome, as well as in evasion of host innate immunity^{10,13}.

After an incubation period of 1 to 3 months, RABV causes neurological signs in humans; there are no effective treatments once the symptoms develop. However, post-exposure prophylaxis (PEP) using rabies vaccine and anti-rabies immunoglobulins, permits survival of infected individuals without clinical symptoms, if initiated soon after exposure^{1,30,35}. In addition, pre-exposure prophylaxis (PrEP) using rabies vaccine also is available for people with occupations engendering a high risk of rabies infection or who travel to areas where rabies is endemic^{1,35,36}.

The Flury strain of RABV, which was isolated from a girl who died of rabies, was adapted to growth in 1-day-old chicks in 1940⁶. Subsequently, the Flury strain was passaged 40–50 times in chicken eggs to generate the low-egg-passage Flury strain (LEP-Flury)^{6,25,26}. The original Flury strain also was passaged 180 times or more in eggs to generate the high-egg-passage Flury strain (HEP-Flury)^{6,25–27}. LEP-Flury has

pathogenicity in adult mice, while HEP-Flury is lethal only in suckling mice, and not in adult mice^{26,28,29}. The purified chick embryo cell vaccine (PCECV) was first produced from the HEP-Flury strain in 1972 and has been manufactured in Japan since 1980^{6,25,30}. Another PCECV developed from the LEP-Flury strain is used in Europe and the USA⁶. In Japan, the chick embryo cell-adapted HEP-Flury small plaque-forming (CEF-S) strain, which was generated by further passages of HEP-Flury in primary chick embryo cells, has been used to produce PCECV²⁵. In Japan, the Rabipur rabies vaccine (GSK Biologicals, Wavre, Belgium) has been licensed for use since 2019. This vaccine, a PCECV derived from LEP-Flury, is imported for use in Japan^{6,37}. However, there are problems in the production of vaccine using primary chicken embryo cells, because preparation of those cells require special techniques and processing time and high costs.

In 1962, the Vero cell line was established from African green monkey kidney cells³⁸. In the late 1970s and early 1980s⁶, an inactivated polio vaccine was produced using the Vero cell line^{39,40}. Subsequently, Vero cell-cultured rabies vaccines were developed in the early 1980s; one such purified Vero cell rabies vaccine (PVRV) has been used in Europe since 1985^{6,13,41}. Among the PVRVs, one is produced using the PV-2061 rabies strain, a virus that has been adapted for growth in Vero cells³⁰. The PV-2061 strain was generated by passage of the Louis Pasteur strain (PV)^{42,43}; passaged 2061 times in rabbit brain, 19

times in the Vero cell line, and five times in baby hamster kidney (BHK) cells⁶. The Verorab rabies vaccine (Sanofi Pasteur, Lyon, France), which is produced using PV-2061^{6,37,44}, and is used world-wide as a PVRV for humans, but this vaccine is not licensed in Japan.

The HEP-Flury strain replicates to high titers in mouse neuroblastoma (MNA) cells as well as neuronal cells^{10,28}, but not in Vero cells⁴⁵. However, the WHO recommends against the use of neuronal cells for the development of human rabies vaccines¹, given that vaccines generated in such cells may induce, in humans, side effects such as acute disseminated encephalomyelitis^{1,46}. In Japan, vaccines against Japanese encephalitis^{47,48} and polio⁴⁰ that were produced in Vero cells have been licensed. In this study, the HEP-Flury strain was adapted to Vero cells to facilitate effective vaccine production, and the functions of amino acid (AA) substitutions induced by adaptation to the Vero cell line were analyzed. Finally, the recombinant virus containing five AA substitutions was produced by reverse genetics as a novel vaccine seed for production of PVRV.

2.3 Materials and Methods

2.3.1 Cells

Vero cells (JCRB9013; Japanese Cancer Research Resources Bank, Tokyo, Japan) were maintained at 37 °C in Dulbecco's modified Eagle's minimum essential medium (DMEM) (Thermo Fisher Scientific, Waltham, MA, USA) supplemented with 5% of heat-inactivated fetal bovine serum (FBS) (Gibco, Grand Island, NY, USA). MNA cells were grown at 37 °C in Eagle's minimum essential medium (MEM) (Thermo Fisher Scientific) supplemented with 10% heat-inactivated FBS. Baby hamster kidney fibroblast (BHK-21) cells were kindly provided by Dr. K. Morimoto (Yasuda Women's University, Hiroshima, Japan) and BHK-21 stably expressing T7 RNA polymerase (BHK/T7-9) cells were provided by Dr. N. Ito (Gifu University, Gifu, Japan)⁴⁹. BHK-21 cells, BHK/T7-9 cells, and human embryonic kidney (HEK-293T) cells (CRL-3216; American Type Culture Collection (ATCC), Manassas, VA, USA) were maintained at 37 °C in MEM supplemented with 10% heat-inactivated FBS.

2.3.2 Viruses

RABV used in this study is our laboratory strain of HEP-Flury (HEP), which historically has been propagated in the MNA cells. The HEP strain originally was stocked

in the Department of Veterinary Science, National Institute of Infectious Diseases, after two rounds of propagation on MNA cells. The complete genomic sequence of our strain, determined as part of the current work, has been deposited in the DNA Data Bank of Japan (DDBJ) as Accession Number: LC785439 (Supplementary Table S1).

2.3.3 Adaptation of HEP-Flury strain to propagation in the Vero cell line

HEP was adsorbed to Vero cells in a T25 flask (Sumitomo Bakelite, Tokyo, Japan) for 1 hour at 37 °C in growth medium (DMEM supplemented with 5% FBS). After adsorption, the cells were incubated in the growth medium for 7 days at 37 °C. The passages of cells were repeated until cytopathic effect (CPE) was observed. After the appearance of CPE, the supernatant was harvested and used as the inoculum for the next passage, as follows: the supernatant was inoculated to 80% confluent Vero cells, and incubated in maintenance medium (DMEM supplemented with 2% FBS) until CPE was again observed. For each such passage, a portion of the supernatant was stored at -80 °C until further use. Virus obtained after 10 and 30 passages in Vero cells was designated HEP-Flury 10V (HEP-10V) and HEP-Flury 30V (HEP-30V), respectively.

2.3.4 Virus titration

Viral titers were determined by a direct fluorescent test using MNA cells. MNA cells (4.0×10^4 cells/well) in 96-well plates incubated at 37 °C with 5% CO₂ for 24 hrs. MNA cells in 96-well plates were inoculated with serial 10-fold dilutions of virus and incubated at 37 °C for 2 days. Cells then were fixed with 80% acetone for 30 min and stained with fluorescein isothiocyanate (FITC) Anti-Rabies Monoclonal Globulin (FUJIREBIO, Tokyo, Japan). Antigen-positive foci were counted under a fluorescence microscope (Nikon, Tokyo, Japan) and quantified as focus-forming unit (FFU) per milliliter.

2.3.5 Comparison of viral growth

Vero cells in 6-well plates were inoculated with each of the RABV strains at a multiplicity of infection (M.O.I.) of 0.05 or 0.01. For the rHEP-10V+V164E, L183P strain's titer was too low to perform the growth curves at an M.O.I. of 0.05. Therefore, Fig 7c was performed at an M.O.I. of 0.01. After 1 hour of adsorption, the cells were washed three times with DMEM and 2 mL of maintenance medium was added to each well. The supernatant was collected at the indicated time points. Each experiment was repeated independently two or three times.

2.3.6 Observation of plaques

Vero cells in 6-well plates were infected with each virus or negative control (medium only) at a M.O.I. of 0.01. After 1 hour of adsorption, the cells were washed three times with DMEM and 2 mL of maintenance medium was added to each well. At the indicated time points, the cells in a given were fixed with 80% acetone and stained with FITC Anti-Rabies Monoclonal Globulin and Evans blue (FUJIFILM Wako Pure Chemical Corporation, Osaka, Japan). The stained cells were visualized under a fluorescence microscope and quantified using NIS-Elements D version 5.20.00 imaging software (Nikon).

2.3.7 Inoculation of rabbits with rabies vaccines

The experimental protocol was approved by the Committee for Animal Experimentation of the National Institute of Infectious Diseases (NIID) (Approval number 120083). All methods were carried out in accordance with relevant guidelines and regulations. All possible efforts were made to minimize the suffering of laboratory animals. During this portion of the animal studies, the rabbits were housed in the animal facility of the NIID. All methods are reported in accordance with ARRIVE guidelines.

Four young adult female Japanese white rabbits (body weight, 2–3 kg) (Kitayama Labes, Nagano, Japan) were inoculated intradermally with commercial rabies vaccines,

consisting of either the “KMB” rabies vaccine (KM Biologics, Kumamoto, Japan) intended for use in animal or the “Rabipur” rabies vaccine intended for use in human. Inoculation was performed every other week for a total of 7 doses, and blood samples were collected 7 days after the last immunization. Rabbits in this study were sacrificed via exsanguination under deep anesthesia by intravenous injection of Pentobarbital.

2.3.8 Challenge experiment in mice with each HEP

The experimental protocol was approved by the Committee for Animal Experimentation of the NIID (Approval number 121021). All methods were carried out in accordance with relevant guidelines and regulations. All possible efforts were made to minimize the suffering of laboratory animals. During this portion of the animal studies, all mice were housed in the animal facility of the NIID. All methods are reported in accordance with ARRIVE guidelines.

Six-week-old ICR (adult) mice (8/group) or suckling mice (10/group) (Japan SLC, Shizuoka, Japan) were inoculated intracerebrally with 10^5 FFU/mouse of HEP, HEP-10V, HEP-30V, or MEM medium (as a negative control “mock”). Body weights of the adult mice were monitored until 21 days post infection (d.p.i.), and mortality was recorded once daily through for 30 d.p.i. adult mice or through 10 d.p.i. suckling mice. At 30 d.p.i., sera

were collected from surviving adult mice. Mice in this study were sacrificed via isoflurane inhalation overdose euthanasia systems, followed by cervical dislocation.

2.3.9 Reverse transcription-polymerase chain reaction (RT-PCR)

RABV RNA was extracted from the supernatant of infected cells using the QIAamp Viral RNA Mini Kit (QIAGEN, Hilden, Germany) according to the manufacturer's protocol. To generate cDNA, RT was performed as follows: 10 μ L of template RNA and 1 μ L of Random-Primers (Promega, Madison, WI, USA) were combined, and the mixture was heated at 95 °C for 1 minute. Subsequently, AMV Reverse Transcriptase (Promega), Recombinant RNasin Ribonuclease Inhibitor (Promega), and dNTP Mixture (TaKaRa Bio, Shiga, Japan) were added, and the mixture then was incubated at 42 °C for 45 minutes before being incubated at 95 °C for 5 minutes. The resulting reverse transcribed cDNA was used for the subsequent PCR amplification of fragments of the RABV genomes.

The cDNA templates were subjected to PCR using Platinum Taq DNA Polymerase High Fidelity (Thermo Fisher Scientific) and the respective primer sets. Detailed information on the PCR conditions and primer sequences are provided in Supplementary Table S7. Amplified products were subjected to gel electrophoresis on 1% agarose to

confirm fragment sizes. The PCR products then were purified using the QIAquick PCR Purification Kit (QIAGEN) and used as templates for DNA sequence analysis.

2.3.10 Sequence analysis

Purified PCR products corresponding to segments of the RABV genome were analyzed by Sanger sequencing method using the BigDye Terminator v3.1 Cycle Sequencing Kit (Thermo Fisher Scientific) followed by separation on an Applied Biosystems 3130xl machine (Thermo Fisher Scientific). Sequence assembly and further analysis was conducted using GENETYX Ver.15 software (GENETYX, Tokyo, Japan).

2.3.11 Rapid fluorescent focus inhibition test (RFFIT)

The VNA titers were determined using a modified RFFIT assay⁵⁰⁻⁵². Briefly, sera were diluted in a 96-well plate 5-fold with MEM containing 2% FBS and an equal volume of virus suspension containing 50 of a 50% focus forming dose (50 FFD₅₀) of RABV then was added to each well. After incubation at 37 °C for 90 min, 100 µL of the mixture was transferred into MNA cells (4.0×10⁴ cells/well) in 96-well plate and incubated at 37 °C with 5% CO₂ for 24 hrs. The controls for this experiment included the WHO reference and negative sera. After 24 hours, the cells were fixed with 80% acetone and stained with

FITC Anti-Rabies Monoclonal Globulin.

2.3.12 Immunoblot analysis

Vero cells in 6-well plates were infected with RABV or negative control (medium) at an M.O.I. of 5. Aliquots of infected cells were harvested each day and lysed with 100 μ L/well of lysis buffer (0.1% sodium dodecyl sulfate, 1% sodium deoxycholate 1% Triton X-100, 10 mM Tris-HCl (pH 7.4), 150 mM sodium chloride, 0.5 mM ethylene diamine tetra acetic acid (EDTA)) on ice for 1 hour. The extracts were centrifuged at 15,000 rpm for 30 min at 4 °C, and the resulting supernatants were stored at -80 °C until use. The concentration of total protein in each supernatant was determined using TaKaRa BCA Protein Assay Kit (TaKaRa Bio) according to manufacturer's instructions. Equal weights of total protein were separated on a NuPAGE 4–12% Bis-Tris Gel (Thermo Fisher Scientific) and transferred to an Immobilon-P Transfer membrane (Thermo Fisher Scientific). After 1 hour of blocking with Blocking One (Nacalai Tesque, Kyoto, Japan), the membrane was reacted at room temperature for 1 hour with primary antibodies consisting of anti-RABV-G (1:200), anti-RABV-N (1:1000), or glyceraldehyde-3-phosphate dehydrogenase (GAPDH) antibody (1:2000) (5G4; Hy Test, Danvers, Turku, Finland). Anti-RABV-G and -N rabbit sera were prepared as described previously⁵³. The

membranes were then washed with Tris-buffered saline-0.05% Tween 20 (BIO-RAD, Hercules, CA, USA) and incubated for 1 hour at room temperature with the following horseradish peroxidase (HRP)-conjugated secondary antibodies: Goat anti-Rabbit IgG (H+L) Secondary Antibody (1:2000) (65-6120; Thermo Fisher Scientific) or Goat Anti-Mouse IgG1 (1:1000) (A90-205P; Abcam, Cambridge, UK). Finally, the membranes were stained with Peroxidase Stain DAB kit (Nacalai Tesque) or Chemi-Lumi One Ultra (Nacalai Tesque). Band intensity was quantified using ImageJ software (National Institutes of Health, Bethesda, MD, USA).

2.3.13 Construction of plasmids for reverse genetics

To construct the infectious clone of RABV, PCR was performed using Prime STAR GXL (TaKaRa Bio) to generate three overlapping PCR amplicons covering the entire RABV genome. Overlapping PCR then was performed with three PCR amplicons using Phusion Hot Start II High-Fidelity DNA Polymerase (Thermo Fisher Scientific) to generate a cDNA representing the full genome. Mutant viruses were constructed by introducing point mutations by PCR using Prime STAR Max (TaKaRa Bio) and synthetic primers with the indicated sequences. Detailed information on the PCR conditions and the primer sequences are provided in Supplementary Tables S8 and S10. The assembled

cDNA containing the sequence of the hammerhead ribozyme sequence (HamRz), the full-length cDNA of RABV genome in the antigenomic orientation, and the hepatitis delta virus ribozyme sequence (HdvRz) was inserted between the *KpnI* and *PstI* sites of the pcDNA3.1 Zeo (+) plasmid (Thermo Fisher Scientific), in parallel to the previously reported constructs^{26,54}. Before the insertion into the cloning vector, the Zero Blunt TOPO PCR Cloning Kit (Thermo Fisher Scientific) was used for sub-cloning.

To construct helper plasmids, the genes encoding the N, P, G, and L proteins were amplified from HEP-Flury using conventional PCR (Supplementary Table S9) and cloned between the *KpnI* and *PstI* sites of the pcDNA3.1 Zeo (+) plasmid. The resulting helper plasmids were designated pH-N, pH-P, pH-G, and pH-L, respectively. Nucleotide sequences of the assembled full-length cDNA clones and of the helper plasmids were confirmed by sequencing.

2.3.14 Rescue of recombinant viruses

BHK-21 or BHK/T7-9 cells (3.0×10^5 cells/well) were grown overnight in 6-well plates in MEM supplemented with 10% FBS. Cells were transfected with per well 1.2 μ g of the full-length plasmid and 450 ng each of pH-N, pH-P, pH-G, and pH-L, and transfection was conducted using the TransIT-LT1 Transfection Reagent (Mirus Bio,

Madison, WI, USA) according to the manufacturer's protocol. After 20–24 hours, the transfection medium was replaced with fresh MEM supplemented with 10% FBS. After 5 days, supernatants were collected and an aliquot of each was inoculated to MNA cells to confirm the presence of the virus as assessed by a fluorescent antibody (FA) test. Supernatants from virus-positive wells were propagated in MNA cells to produce virus stock. Nucleotide sequences of all rescued viruses were confirmed by sequencing.

2.3.15 Comparison of efficiency of cell infection

The FFU of the recombinant viruses were determined by plating in MNA cells. The resulting values were used to generate serial 2-fold dilutions of recombinant viruses starting from 1000 FFU/well, and these dilutions were used as inoculation to infect MNA or Vero cells in 12-well plates. After 1 hour of adsorption, the cells were washed three times with MEM and medium containing 1% methyl cellulose was added at 1 mL/well, and the resulting cultures were incubated for 2 days. The cells then were fixed for 30 min with 10% formalin solution containing 0.4% Triton X-100 (Merck, Darmstadt, Germany) and stained with FITC Anti-Rabies Monoclonal Globulin. Antigen-positive foci were counted under a fluorescence microscope. The ratio of the number of foci in Vero cells to that in MNA cells was calculated in the well which inoculated with 500 FFU/well.

2.3.16 Flow cytometric analysis

Vero cells in 6-well plates were infected with viruses or negative control (medium “mock” infection) at an M.O.I. of 5 and incubated for 2 days. The infected cells were washed with phosphate-buffered saline (PBS) and released by treatment with 2.9 mM EDTA. The cells were collected, washed with sorting buffer, and reacted for 1 hours on ice with the mouse monoclonal anti-RABV G antibody #7-1-9⁵³ (0.4 mg/mL) (1:80). Cells were then washed twice and reacted for 1 hour on ice with the FITC-conjugated Goat Anti-Mouse IgG1 secondary antibodies (1:1600) (FI-2000; Vector Laboratories, Newark, CA, USA). Next, the cells were washed twice and fixed at room temperature for 20 minutes in 4% paraformaldehyde. Finally, the cells were again washed twice and sorted using a BD FACS Canto II flow cytometer (Becton Dickinson and Company; BD, Franklin Lakes, NJ, USA) with blue lasers (488nm) for the detection of FITC. The resulting data were analyzed using Kaluza Analysis Software Version 2.1 (Beckman Coulter Life Sciences, Indianapolis, IN, USA).

2.3.17 Production of pseudotyped vesicular stomatitis virus (VSVp)

Secreted alkaline phosphatase (SEAP)-expressing VSVp particles that were

pseudotyped with HEP, HEP-10V, or HEP-30V G proteins were produced as described previously⁵⁵. Briefly, an expression plasmid encoding the RABV G protein was transfected into 80% confluent HEK293T cells using polyethylenimine (Thermo Fisher Scientific) according to the manufacturer's instructions. At 2 d.p.i., the cultures were inoculated with VSV Δ G-SEAP (a kind gift of Dr. Y. Matsuura, Osaka University, Japan) at an M.O.I. of 1. After 1 hour of adsorption, the HEK293T cells were washed three times with MEM and MEM containing 2% FBS was added to each well. After 24 hours, the culture supernatants were harvested and filtered through gamma-sterilized Millex-HV Syringe Filter Units, (0.45 μ m pore size, polyvinylidene fluoride (PVDF) membrane, 33 mm diameter) (Thermo Fisher Scientific). These resulting virus suspensions were stored at -80 °C until use.

2.3.18 Titration of VSVp

To determine the infectious titer of the VSVp stocks, MNA cells in 96-well plates were inoculated with serial 2-fold dilution of the VSVp suspensions. After 1 hour of adsorption, MNA cells were washed three times with MEM and MEM containing 2% FBS was added at 100 μ L/well. After overnight incubation, cells were fixed with 80% acetone for 30 minutes and incubated for 1 hour at 37 °C with mouse anti-VSV

nucleoprotein antibody (1:1000) (MABF2348; Thermo Fisher Scientific) as the primary antibody. After three washes, cells were stained with FITC-conjugated goat anti-mouse IgG (H&L; 1:200) (ab6785; Abcam) as the secondary antibody.

2.3.19 Quantification of infection with VSVp

Serial 2-fold dilutions of VSVp stocks were inoculated to MNA or Vero cells and adsorbed for 1 hour. The cells then were washed three times with MEM or DMEM, and MEM or DMEM supplemented with 2% FBS was added at 100 μ L/well. After overnight incubation at 37 °C, an aliquot 40 μ L of each culture supernatant was transferred to a new 96-well plate, to which substrate solution (SIGMAFAST p-Nitrophenyl Phosphate Tablets, Thermo Fisher Scientific) was added at 200 μ L/well. After the plates were incubated for 2 hours at 37 °C, the amount of SEAP was determined by measuring the optical density at a wavelength of 405 nm (OD405) using a spectrophotometer (iMarkTM Microplate Absorbance Reader, BIO-RAD).

2.3.20 Statistical analysis

Unless otherwise indicated, data are presented as the mean \pm standard deviation (S.D.). Statistical analyses were conducted using a one-way Analysis of Variance

(ANOVA) with post hoc Tukey's multiple-comparison tests or the two-way ANOVA followed by either Tukey's, Dunnett's or Sidak's multiple-comparison tests. A log-rank test was used to analyze the Kaplan-Meier survival curves. Analyses were performed using in GraphPad Prism9 (GraphPad Software, San Diego, CA, USA). Values of $p < 0.05$ were considered statistically significant.

2.4 Results

2.4.1 Adaptation of HEP-Flury to Vero cells

Before adaptation of our HEP-Flury (HEP) to Vero cells, we determined the complete genome sequence of the HEP strain used in our laboratory and compared that sequence to those reported for other HEP-Flury strains (Supplementary Table S1). The genome of our strain was most similar to that previously reported⁵⁴ as HEP-Flury strain Accession Number AB085828, and had only one AA substitution in the signal peptide of G protein. The CEF-S strain (Accession No. LC717412), which is propagated in chick embryo fibroblast cells and is used as the Japanese vaccine strain, had twenty AA substitutions compared to our HEP: four substitutions in the P protein, three substitutions in the M protein, nine substitutions in the G protein and four substitutions in the L protein.

In the present study, we sought to adapt our HEP strain to Vero cells to facilitate efficient vaccine production in this cell line. To this end, HEP was subjected to 30 rounds of serial passages in Vero cells. At passages 1 and 2, the infected Vero cells were blindly passaged because CPE was not observed. At passage 3, CPE was observed at 6 d.p.i. and all subsequent viral passages consisted inoculation of the culture supernatants into Vero cells. From passages 4 to 17, HEP caused CPE at 3 d.p.i., and from passage 18, CPE was observed at 2 d.p.i.

2.4.2 Comparison of viral growth of HEP and adapted HEPs in Vero cells

To compare viral growth among the adapted HEP strains, Vero cells were infected at M.O.I. of 0.05 with HEP or the adapted strains that had been passaged 10 and 30 times in Vero cells, designated HEP-10V and HEP-30V, respectively (Fig. 1a and Supplementary Table S2). HEP-10V and HEP-30V accumulated to significantly higher titers than HEP did when grown in Vero cells, as assessed at 1–4 d.p.i. (HEP-10V; $p=0.046$, 0.031 , 0.002 , HEP-30V; $p=0.047$, 0.001 , <0.001 , <0.001 , respectively). Additionally, HEP-30V accumulated to titers that were nominally higher than those of HEP-10V when grown in Vero cells without statistical significance.

To visualize differences in viral spread when propagated in Vero cells, HEP, HEP-10V, and HEP-30V were infected to Vero cells at an M.O.I. of 0.01, and the infected cells were fixed and stained with FITC-conjugated anti-RABV antibody at 1–4 d.p.i. (Fig. 1b). For those cells, RABV-positive cells were observed at 2 d.p.i. However, the number of infected cells increased more rapidly in HEP-10V- and HEP-30V-infected cells than in HEP-infected cells, and the number of infected cells increased more rapidly in HEP-30V-infected cells than in HEP-10V-infected cells.

2.4.3 Comparison of expression of viral proteins by HEP and the adapted HEPs

To compare the expression levels of the viral proteins, immunoblot analysis was performed using anti-rabies G and N antibodies (Fig. 2a and Supplemental Figure S1), and for comparison, values were normalized to those of the housekeeping protein, GAPDH (Fig. 2b). In HEP-infected cells, G and N proteins were detected from 1 d.p.i., but afterwards the amounts subsequently did not change appreciably up to 4 d.p.i. On the other hand, in HEP-10V- and HEP-30V-infected cells, expression of the G and N proteins appeared to increase from 2–4 d.p.i. The expression of those proteins in HEP-10V- and HEP-30V-infected cells were significantly increased from 2–4 d.p.i. compared in HEP-infected cells ($p<0.001$). Notably, the N protein accumulated to significantly higher levels in HEP-30V-infected cells than in HEP-10V-infected cells at 2 and 3 d.p.i. ($p=0.02$ and $p<0.001$).

2.4.4 Comparison of antigenicity between HEP and Vero-adapted HEPs

To compare the antigenicity of the parent and adapted viruses, RFFITs were performed using sera obtained from four rabbits (H1, H2, A1, and A2) (Fig. 3). The H1 and H2 sera were collected from rabbits vaccinated with a human rabies vaccine (Rabipur) and the A1 and A2 sera were collected from rabbits vaccinated with an animal

rabies vaccine (KMB). Although a statistically significant difference in VNA titers was observed between HEP and HEP-30V ($p=0.048$) using one serum (H1), statistically significant differences were not detected for any comparisons using other tested sera.

2.4.5 Comparison of pathogenicity between HEP and adapted HEPs

To compare the pathogenicity of HEP and the adapted strains, 10^5 FFU of HEP, HEP-10V, and HEP-30V were inoculated intracerebrally into suckling ICR mice (Fig. 4a) and 6-week-old adult ICR mice (Fig. 4b). Suckling mice infected with HEP or HEP-10V began to show neurological signs (such as tremors and paralysis) at 4 d.p.i., subsequently dying at 6–9 d.p.i. However, HEP-30V-infected suckling mice presented neurologic signs at 5 d.p.i., subsequently dying at 6–10 d.p.i. For all strains, all infected adult mice survived until 30 d.p.i., and showed no clinical signs other than body weight loss. Among the inoculated adult mice, body weights monitored through 21 d.p.i., in those infected with HEP exhibited a mean loss of weight (compared to baseline) of 10.6% at 7 d.p.i. before subsequently recovering. In contrast, HEP-10V- or HEP-30V-infected mice exhibited mean weight losses of 4.0% or 2.6%, respectively, at 7 d.p.i. before subsequently recovering.

2.4.6 Comparison of VNA activity using sera from mice infected with HEP or adapted HEPs

Serum was collected from mice inoculated with each of the viral strains. Since the amounts of serum from individual mice were not sufficient for the tests, equal volume of sera from each mouse from a given group were pooled for analysis by RFFIT (Fig. 4c). Sera from mice infected with HEP showed that nominally highest VNA titers against HEP, with the differences achieving statistical significance against HEP-10V ($p=0.020$). In sera from HEP-10V- and HEP-30V-infected mice, there was no significant difference in VNA titers against HEP, HEP-10V, or HEP-30V.

2.4.7 Comparison of the viral genomes among HEP, HEP-10V, and HEP-30V

Sequence analysis revealed that the nucleotide sequences of HEP-10V (Accession No. LC785440) and HEP-30V (Accession No. LC785441) exhibited 99.97% and 99.94% identity to those of HEP (Accession No. LC785439). All of the observed changes were missense; no silent mutations were detected. The positions of AA substitutions in the viral genome are indicated in Fig. 5a, and included totals of 3 and 7 AA substitutions for the proteomes of HEP-10V and HEP-30V, respectively (Fig. 5b). In HEP-10V, one AA substitution each was found in the P, G, and L proteins. In HEP-30V, a further three AA

substitutions were found in the G protein, as well as one AA substitution in the L protein.

2.4.8 Comparison of viral growth in Vero cells of recombinant HEP and HEP-10V viruses

To determine which substitutions are responsible for the adaptation of viral growth in Vero cells, we employed reverse genetics to construct eight recombinant viruses corresponding to HEP, HEP-10V and HEP with each of one or two mutations (Fig. 6a). The resulting recombinant viruses were inoculated into Vero cells at an M.O.I. of 0.05, and viral growth was compared by measuring viral titers at multiple time points (Fig. 6b and Supplementary Table S3). Among the tested strains, the recombinant HEP (rHEP) strain showed the lowest titers during propagation in Vero cells. rHEP-10V(L), which had L(D2055E) in the L protein, yielded titers that were statistically indistinguishable from those of the parent rHEP. rHEP-10V(G), which had G(S15R) in the mature G protein, and the rHEP-10V(G,L), which had both G(S15R) and L(D2055E), yielded titers that were nominally higher than those obtained with rHEP, although the differences were not statistically significant. On the other hand, rHEP-10V(P), which had P(L115H) in the P protein, and rHEP-10V(P,L), which had both P(L115H) and L(D2055E), yielded titers that were significantly higher than those of rHEP ($p < 0.001$) at all assessed time points.

The rHEP-10V(P,G), which had both P(L115H) and G(S15R), yielded titers that were nominally higher than those of rHEP-10V(P) and rHEP-10V(P,L). Titers obtained from rHEP-10V(P,G) were statistically indistinguishable from those obtained from rHEP-10V. Interestingly, cultures of both rHEP-10V(P,G) and rHEP-10V showed CPE at 3 or 4 d.p.i. in Vero cells, an observation not seen with the other recombinant viruses (data not shown).

2.4.9 Comparison of virus entry in Vero cells by recombinant viruses

To compare the efficiency of entry by recombinant viruses, rHEP-10V(P) with P(L115H) and rHEP-10V(G) with G(S15R) were used to infect both Vero and MNA cells and following adsorption, the infected cells were overlaid with methylcellulose medium. Following staining with FITC-conjugated anti-rabies virus antibody, the cultures were analyzed for the number of foci, and the ratio of foci in the two cell lines was calculated (Fig. 6c). This analysis demonstrated that the entry of rHEP-10V(P) and rHEP-10V into Vero cells were statistically significantly more efficient than that of rHEP and rHEP-10V(G) ($p < 0.001$). On the other hand, the entry of rHEP-10V(G) into Vero cells was statistically indistinguishable from that of rHEP.

To examine the role of the G(S15R) substitution, viral entry was assessed using SEAP-expressing VSVp pseudotyped with the G protein of either HEP or HEP-10V.

Before initiation of this experiment, we tittered the number of particles of the VSVp stock by inoculating MNA cells and detecting particles by indirect fluorescence assay using anti-VSV N antibody. Based on these titers, Vero cells were inoculated with a series 2-fold dilution of each VSVp starting from 150 particles per well. The results showed that similar rates of Vero cell entry were observed with recombinant VSVp pseudotyped with the parental HEP or the adapted HEP-10V G protein (Fig. 6d).

2.4.10 Comparison of cell surface accumulation of viral proteins by recombinant

HEP-Flury strains

The results described above showed that rHEP-10V(P) entered Vero cells more efficiently than rHEP, which could not be attributed to differences in the G protein sequence. We hypothesized that the observed difference in entry efficiency might be attributable to the amount of G protein on the viral particles when comparing among recombinant viruses. To assess the level of G protein on the surfaces of Vero cells, the recombinant viruses rHEP, rHEP-10V(G), rHEP-10V(P), rHEP-10V(P,G), and rHEP-10V, were inoculated to Vero cells at an M.O.I. of 5. At 2 d.p.i., the infected cells were collected and stained with anti-rabies G protein monoclonal antibody (#7-1-9). Analysis by fluorescence-activated cell sorting (FACS) showed that the level of G protein displayed

on the cell surface was highest in rHEP-10V(P,G)-infected cells, followed by those in rHEP-10V-, rHEP-10V(P)-, rHEP-10V(G)-, and rHEP-infected cells (Fig. 6e). In the rHEP-infected cells, the amount of G protein displayed was lower as well as that in mock-infected cells ($p=0.815$), while that on rHEP-10V(P)-infected cells exceeded those on rHEP-10V(G)- ($p=0.095$) and rHEP-infected cells ($p=0.012$). Interestingly, the level of G protein on rHEP-10V(P,G)-infected cells was significantly greater more than that in rHEP-10V(P)-infected cells ($p=0.044$).

2.4.11 Comparison of viral growth among recombinant HEP-10V with each mutation in HEP-30V

Compared to HEP-10V, HEP-30V harbors 4 additional mutations, resulting in three AA substitutions in the G protein, G(V164E), G(L183P), and G(A286V), and one AA substitution in the L protein, L(E753D). To investigate the effect of these substitutions on viral growth, we generated recombinant viruses using reverse genetics to introduce these HEP-30V mutations into the genome of HEP-10V (Fig. 7a). In an initial experiment, we compared the viral growth of rHEP-10V, rHEP-10V harboring the single mutation in the L protein (rHEP-10V+L1), rHEP-10V harboring the triad of mutations in the G protein (rHEP-10V+G3), and rHEP-30V (Fig. 7b and Supplementary Table S4). The results

indicated that the change in the L protein did not affect viral growth, while the three mutations in the G protein, whether in rHEP-10V+G3 or in rHEP-30V, provided significantly enhanced viral growth compared to the rHEP-10V parent (rHEP-10V+G3; $p=0.028$, rHEP-30V; $p=0.001$, 0.039 , respectively).

Next, recombinant viruses harboring individual or paired mutations in the G protein were constructed (Fig. 7a) and their viral growth was compared to that of the rHEP-10V parent (Fig. 7c and Supplementary Table S5). Among the resulting mutants, only the V164E, A286V double mutant (rHEP-10V+V164E, A286V) exhibited significantly more efficient growth than rHEP-10V ($p=0.049$, 0.003 , 0.010 , and 0.014 , respectively), and the other recombinant viruses with single or double substitutions grew as well as rHEP-10V. However, the viral growth of rHEP10V+V164E, A286V was significantly attenuated compared to those of rHEP-30V at 3 d.p.i. ($p=0.036$).

2.4.12 Comparison of viral entry using VSVp pseudotyped with the G protein of HEP-30V

Recombinant viruses rHEP-10V+G3 and rHEP-30V, both of which harbored three mutations in the G proteins exhibited significantly improved growth compared to rHEP-10V (Fig. 7c). As above, we compared viral entry efficiencies using SEAP-expressing

VSVp pseudotyped with the G protein of either HEP-10V or HEP-30V. The results indicated that the VSVp pseudotyped with the HEP-30V G protein entered Vero cells with significantly greater efficiency than did VSVp pseudotyped with HEP G protein ($p=0.029$) or with the HEP-10V G protein ($p=0.006$) (Fig. 7d).

2.4.13 Comparison of viral growth among recombinant viruses with five mutations

In the experiments described above, we determined that mutations resulting in five substitutions (P(L115H), G(S15R), G(V164E), G(L183P) and G(A286V)) all contributed to the potentiation of growth efficiency in Vero cells. To confirm these results, we constructed a recombinant virus, designated rHEP-PG4, that carries all five of these mutations (Fig. 8a) and assessed the viral growth of this strain in Vero cells (Fig. 8b and Supplemental Table S6). We observed that the growth of rHEP-PG4 was statistically indistinguishable from those of rHEP-10V+G3 and rHEP-30V. This result showed that this rHEP-PG4 strain represents a version of HEP-Flury with the minimum number of mutations sufficient for Vero cell adaptation. To compare the antigenicity of the rHEP and rHEP-PG4, RFFITs were performed using four rabbits sera (H1, H2, A1, and A2) (Fig. 8c). There was no statistically significant differences in VNA titers against rHEP and rHEP-PG4.

2.5 Discussion

In the present study, we succeeded in producing two Vero cell-adapted HEP-Flury strains, HEP-10V and HEP-30V. These strains had similar or lower pathogenicities than the parent HEP (Fig. 4a, b), and their antigenicities were similar to that of the parent (Figs. 3 & 4c). Nucleotide sequence analysis showed that the HEP-10V harbored mutations resulting in 3 AA substitutions, including P(L115H), G(S15R), and L(D2055E). HEP-30V carried additional mutations, which resulted in another three substitutions in the G protein, G(V164E), G(L183P) and G(A286V), and a single substitution in the L protein, L(E753D) (Fig. 5). This HEP-30V harboring a total of seven substitutions (compared to the parent, HEP) should be considered a candidate for use as a seed for vaccine production in Vero cells, given its adaptation to growth in Vero cells while exhibiting pathogenicity and antigenicity similar to those of the HEP parent.

Next, we examined the mechanism of adaptation by analysis of recombinant HEP carrying individual mutations. The recombinant viruses rHEP-10V(P), rHEP-10V(P,L), rHEP-10V(P,G), and rHEP-10V, which carried a mutation in the P protein resulting in P(L115H) substitution, showed significantly better growth in Vero cells than did the strains lacking this mutation (rHEP, rHEP-10V(L), rHEP-10V(G) and rHEP-10V(G,L), respectively) (Fig. 6b and Supplementary Table S3). These results indicated that the

P(L115H) substitution supports adaptation of HEP to growth in Vero cells. In addition, the rHEP-10V(P) demonstrated significantly more efficient entry into Vero cells than rHEP (Fig. 6c), indicating that the P(L115H) substitution potentiated effective viral entry. Furthermore, the amount of the G protein on the cell surface was increased in cells infected by virus harboring the mutation causing the P(L115H) substitution (Fig. 6e). Taken together, these results suggest that the P(L115H) substitution may increase the efficiency of cell entry by promoting the accumulation of the G protein on the cell surface and presumably on the surface of the resulting virus particle.

P protein has at least six major functions¹³ and one of which interacted with focal adhesion kinase (FAK) to regulate RABV infection^{13,56}. FAK is a cytoplasmic tyrosine kinase that localizes to cellular focal contacts and plays important roles in cellular signaling pathways that are involved in the regulation of transcription, the progression of the cell cycle, the modulation of apoptosis, the control of cell migration, and the metastasis of transformed cells⁵⁶⁻⁵⁸. During RABV infection, FAK enhances viral growth by interacting with the P protein, leading to enhancement in the replication and/or translation of the viral RNA⁵⁶. Within the P protein, AA residues between 106 and 131 have been associated with FAK binding; residues R106, R109, R113, F114, W118, and I125 are known to be required for this interaction⁵⁶. The present work indicated a role for

P protein residue 115, although there are no reports of a possible function for this AA. We conjecture that this residue may participate in the interaction between FAK and the P protein, such that the P(L115H) substitution enhances the accumulation of G protein on the surface of RABV-infected Vero cells. Further experiments will be required to clarify the role of the P(L115H) substitution in RABV adaptation to the Vero cell line.

To confirm the reproducibility of these adaptations, recombinant HEP was inoculated into Vero cells and passaged using the same method. The recombinant HEP strain also showed CPE at passage 3, and then the supernatant was inoculated Vero cells for repeated passaging. rHEP passaged 10 times also harbored a total of three missense mutations. While these changes corresponded to one substitution each in the P, G, and L proteins, the positions of the substitutions differed from HEP-10V. Specifically, this strain (rHEP passaged 10 times) substitutions consisted of P(V105D), G(D211N), and L(K875T). The P(V105D) substitution would lie close to the substitution at residue 115 that was observed in HEP-10V. We infer that a domain of the P protein spanning residues 105 to 115 is important for the adaptation of RABV to growth in Vero cells.

The recombinant viruses rHEP-10V(G), rHEP-10V(G,L), rHEP-10V(P,G), and rHEP-10V, which carried a mutation in the G protein resulting in G(S15R) substitution, showed better growth in Vero cells than the strains lacking this mutation (rHEP, rHEP-

10V(L), rHEP-10V(P) and rHEP-10V(P,L), respectively) (Fig. 6b and Supplemental Table S3). On the other hand, no significant difference in entry was detected between rHEP and rHEP-10V(G), or between VSVp particles pseudotyped with G proteins from HEP and HEP-10V (Fig. 6c, d). We also observed that G protein accumulated to higher levels on the surface of Vero cells infected with recombinant viruses encoding the G(S15R) mutant protein (rHEP-10V(G) and rHEP-10V(P,G)) than on those infected by viruses lacking this mutation (rHEP and rHEP-10V(P), respectively) (Fig. 6e). Together, these results indicated that the G(S15R) substitution plays important roles in the adaptation of viral growth to Vero cells and in the accumulation of G protein on the cell surface, but does not provide any change in viral entry. We hypothesize that the G(S15R) substitution enhances viral budding from the surface of Vero cells by increasing the amount of G protein accumulating on the cell surface. Further analysis will be needed to resolve the role of the G(S15R) substitution in RABV propagation in Vero cells.

Compared to HEP-10V, HEP-30V had three additional AA substitutions including G(V164E), G(L183P) and G(A286V). rHEP-10V with all three substitutions, rHEP-10V+G3, grew better in Vero cells than strains lacking these mutations (rHEP-10V and rHEP-10V+L1) (Fig. 7b and Supplemental Table S4). In addition, VSVp particles pseudotyped with the G protein of HEP-30V exhibited more-efficient entry into Vero cells

than those of HEP and HEP-10V (Fig. 7d). Recombinant viruses with only one or two of substitutions in the G protein exhibited growth in Vero cells similar to that seen with rHEP-10V (Fig. 7c and Supplemental Table S5). Only rHEP-10V+V164E, A286V exhibited growth in Vero cells that was significantly better than that seen with rHEP-10V, while this strain did less than by rHEP-10V+G3 and rHEP-30V. These results indicated that all three substitutions play important roles in viral growth, and that these changes are mediated by effects on virus entry.

The mature G protein consists of three domains (ectodomain, transmembrane domain and cytoplasmic domain)¹³, and all of the G protein substitutions identified in HEP-30V in the present work are located in the ectodomain. G protein residues 164, 183, and 286 have not identified as part of a pathogenicity-related site^{26,59-61}, epitope site^{62,63}, *N*-glycosylation site^{53,60,62,64}, or cell receptor-binding site^{11,65}. Other work has shown that the G protein recognizes and adheres to neuronal cell receptors such as heparin sulfate⁶⁶, the acetylcholine receptor (nAChR)⁶⁷, the neural cell adhesion molecule (NCAM)⁶⁸, the low-affinity neurotrophic receptor (p75NTR)⁶⁹ and the metabotropic glutamine receptor subtype II (mGluR2)⁷⁰. In the present study, the G(V164E), G(L183P), and G(A286V) substitutions were associated with enhanced entry into Vero cells. Notably, Vero cells are known to display two receptors, NCAM and heparan sulfate, on the cell surface^{68,71}. To

our knowledge, the site within the G protein that is responsible for receptor-binding to NCAM has not been reported yet. On the other hand, the G protein site responsible for binding to the heparan sulfate receptor has been reported to be located at residues 126 to 273⁶⁶. Therefore, two of the identified here (G(V164E) and G(L183P)) may contribute to changes in heparan sulfate binding by the G protein. In addition, in silico structural modeling of the G protein using Molecular Operating Environment software version 2022.02 (Chemical Computing Group, Montreal, Canada)⁷² suggests that residues 164 and 183 are located at conformationally related positions on the protein, whereas residue 286 is predicted to be located internal to the protein (not shown). Therefore, the G(V164E) and G(L183P) substitutions are candidates for sites that might enhance the binding of the G protein to cell receptors displayed on Vero cells, including heparan sulfate and other unknown receptors.

In comparison with the other Vero-adapted RABV isolate, strain PV-2061, a single amino acid residue proline (P) at position of 183 of the G protein of PV-2061 was identical to G(L183P) of HEP-30V. However, this proline at position of 183 is conserved in the parental strain PV and the other street viruses. In HEP, this amino acid is important for Vero adaptation, but it may have a different role in the other strains. Interestingly, PV-2061 has a P(L115F) substitution in the P protein in comparison with the parent strain PV.

Since the substitution P(L115H) in HEP plays an important role in viral growth in Vero cells, the P(L115F) substitution might enhance viral growth of PV-2061 in Vero cells. Further experiments will be required to clarify the role of the P(L115H) substitution in the adaptation of RABV to the Vero cell line.

Thus, in the present work, we generated recombinant HEP-Flury by reverse genetics and demonstrated that the combination of five AA substitutions (P(L115H), G(S15R), G(V164E), G(L183P) and G(A286V)) were sufficient for the adaptation of this RABV strain to growth in Vero cells. This recombinant RABV, which have designated rHEP-PG4, is not different compared to rHEP in their antigenicity. Above all, rHEP-PG4 is expected to serve as a candidate seed virus for propagation in Vero cells for vaccine production.

2.6 Figure legends

Fig. 1. Viral growth and spread of HEP-Flury (HEP) and Vero-adapted viruses (HEP-10V and -30V) in Vero cells

Vero cells were inoculated with HEP, HEV-10V, or HEV-30V at a multiplicity of infection (M.O.I.) of 0.05. Supernatants were collected once daily through 4 days post infection (d.p.i.). (a) Viral titers were determined using MNA cells. Antigen-positive foci were counted under a fluorescence microscope and quantified as focus forming unit (FFU) per milliliter. Viral titers are plotted as the mean and standard deviation (S.D.) from three independent experiments. Significant differences are indicated (*: $p < 0.05$, **: $p < 0.01$, ***: $p < 0.001$) between HEP and HEP-10V or HEP-30V after application of two-way ANOVA followed by Tukey. HEP-10V vs HEP-30V had no significant difference at all time points ($p > 0.05$). (b) At the indicated time points, virus- and mock-infected cells were fixed with 80% cold acetone. Fixed cells were stained with the fluorescein isothiocyanate (FITC) anti-rabies monoclonal globulin (FUJIREBIO, Tokyo, Japan) and examined under a fluorescence microscope. The stained cells were observed using NIS-Elements D version 5.20.00 imaging software (Nikon, Tokyo, Japan). Cells are stained red with Evans Blue (FUJIFILM Wako Pure Chemical Corporation, Osaka, Japan). Scale bars, 100 μm ; magnification, $\times 40$

Fig. 2. Comparison of expression of viral proteins among HEP, HEP-10V and HEP-30V in Vero cells

Vero cells were inoculated with each virus at an M.O.I. of 5 and harvested every day.

(a) Rabies virus (RABV) glycoprotein (G protein) and nucleoprotein (N proteins) were visualized using polyclonal rabbit anti-serum against each protein. Glyceraldehyde-3-phosphate dehydrogenase (GAPDH), a housekeeping gene, was detected by monoclonal mouse antibody for use as a loading control. (b) Virus-specific bands were quantified using ImageJ software (National Institutes of Health, Bethesda, MD, USA) and levels of RABV G and N proteins were normalized to those of GAPDH. The means and S.D. were calculated from two independent experiments. Significant differences are indicated (*: $p < 0.05$, **: $p < 0.01$, ***: $p < 0.001$) after application of two-way ANOVA followed by Tukey.

Fig. 3. Comparison of virus-neutralizing antibody titers against HEP, HEP-10V and HEP-30V using vaccinated rabbit sera

Sera were collected from each of four rabbits (H1, H2, A1, A2). H1 and H2 were inoculated with the human-RABV vaccine (Rabipur, GSK Biologicals, Wavre, Belgium)

and A1 and A2 were inoculated with the animal-RABV vaccine (KMB, KM Biologics, Kumamoto, Japan). Virus-neutralizing antibody (VNA) titers were determined by rapid fluorescent focus inhibition tests (RFFITs) and quantified using the World Health Organization (WHO) international units (IU/ml). Means and S.D. were calculated from four independent experiments. Significant difference is indicated (*: $p < 0.05$) in the neutralizing activities against HEP and HEP-30V in the H1 rabbit serum after application of two-way ANOVA followed by Tukey.

Fig. 4. Comparison of pathogenicity among HEP, HEP-10V and HEP-30V in suckling and 6-week-old mice, and VNA titers against HEP-Flury using sera pooled from each infected-adult mice group

Suckling (n=10/group) and 6-week-old mice (n=8/group) were inoculated by intracerebral injection with 10^5 FFU per mouse of the respective virus, or with an equivalent volume of medium (mock). Plots show the survival rate of suckling mice using a Kaplan-Meier plot (a) and relative body weights (normalized to baseline) of 6-week-old mice (b). Body weight data are presented as mean and error bars represent the S.D. of each group. (c) The mouse sera were collected from surviving 6-week-old mice which were infected by intracerebral route with HEP, HEP-10V or HEP-30V. VNA titers were

determined by RFFIT and VNA titers are quantified using IU/ml. Means and S.D. was calculated from three independent experiments. Error bars represent the S.D. of each group. Significant difference is indicated (*: $p < 0.05$) in the neutralizing activity between HEP vs HEP-10V on the inoculated HEP mice group after application of two-way ANOVA followed by Tukey.

Fig. 5. Comparison of amino acid sequences between HEP, Vero-adapted viruses and recombinant viruses

(a) Schematic of the rabies genome and rectangles indicate the open reading frames for the indicated proteins. Change of amino acids and their positions are shown by arrow heads. (b) Sequence details of the adapted viruses that are described in the present study. Amino acids are indicated by the standard one-letter abbreviations.

*: Amino acid sequence identical with HEP.

** : Amino acid positions are numbered based on the mature G protein without signal peptide.

Fig. 6. Efficiency of viral growth, entry, and expression of G protein of each recombinant viruses in Vero cells

(a) Information on recombinant viruses used in this figure. *: Amino acid sequence identical with rHEP. **: Amino acid positions are numbered based on the mature G protein without signal peptide. (b) Vero cells were inoculated with the indicated recombinant viruses (a) at a M.O.I. of 0.05 and supernatants were collected every day until 4 d.p.i. Viral titers were determined in MNA cells. (c) The total number of focuses was determined by counting the number of focuses stained with the FITC anti-rabies monoclonal globulin in Vero or MNA cells under a fluorescence microscope. The ratio of the number of focuses in Vero to that in MNA was compared. (d) The particle titer of each secreted alkaline phosphatase (SEAP)-expressing pseudotyped vesicular stomatitis virus (VSVp) stock was determined in MNA cells. Vero cells then were inoculated with 2-fold serial dilutions (starting from 150 particles) of VSVp pseudotyped with the HEP or HEP-10V G protein SEAP activity was assessed in culture supernatants and detected by optical density (OD). (e) Vero cells were inoculated with each recombinant virus at an M.O.I. of 5 and harvested at 2 d.p.i. The cells were stained with anti-rabies G protein monoclonal antibody (#7-1-9) and FITC-conjugated anti-mouse secondary. After that, cells were fixed with 4% paraformaldehyde, and finally analyzed by BD FACS Canto II flow cytometer (Becton Dickinson and Company; BD, Franklin Lakes, NJ, USA) and Kaluza analysis software Version 2.1 (Beckman Coulter Life Sciences, Indianapolis, IN, USA). Data are

presented as the mean and S.D. from three (b,d,e) or four (c) independent experiments. Significant differences are indicated in the comparison between rHEP and each recombinant virus after application of two-way ANOVA followed by Tukey (b), or each virus after application of one-way ANOVA followed by Turkey (c,e) or two-way ANOVA followed by Sidaks (d) (*: $p < 0.05$, **: $p < 0.01$, ***: $p < 0.001$).

Fig. 7. Comparison of viral growth in Vero cells among recombinant HEP strains, and entry of VSVp pseudotyped with the G protein of HEP, HEP-10V or HEP-30V

(a) Information on recombinant viruses used in this figure. *: Amino acid sequence identical with rHEP. **: Amino acid positions are numbered based on the mature G protein without signal peptide. Four recombinant viruses were infected to Vero cells at an M.O.I. of 0.05 (b), while nine recombinant viruses were inoculated at an M.O.I. of 0.01 (c). Viral titers were determined in MNA cells. The means and S.D. of the log₁₀ of the viral titers are calculated from three independent experiments. Significant differences are indicated in the comparison between rHEP-10V and recombinant viruses after application of two-way ANOVA followed by Tukey (*: $p < 0.05$, **: $p < 0.01$, ***: $p < 0.001$). (d) Vero and MNA cells then were inoculated with 150 particles of VSVp pseudotyped with the G protein of HEP, HEP-10V, or HEP-30V. Following growth, SEAP activity was assessed

in culture supernatants and detected by OD value, and the ratio of values in Vero and MNA cells was calculated. Means and S.D. were calculated from four independent experiments. Significant differences are indicated (*: $p < 0.05$, **: $p < 0.01$) after application of one-way ANOVA followed by Tukey.

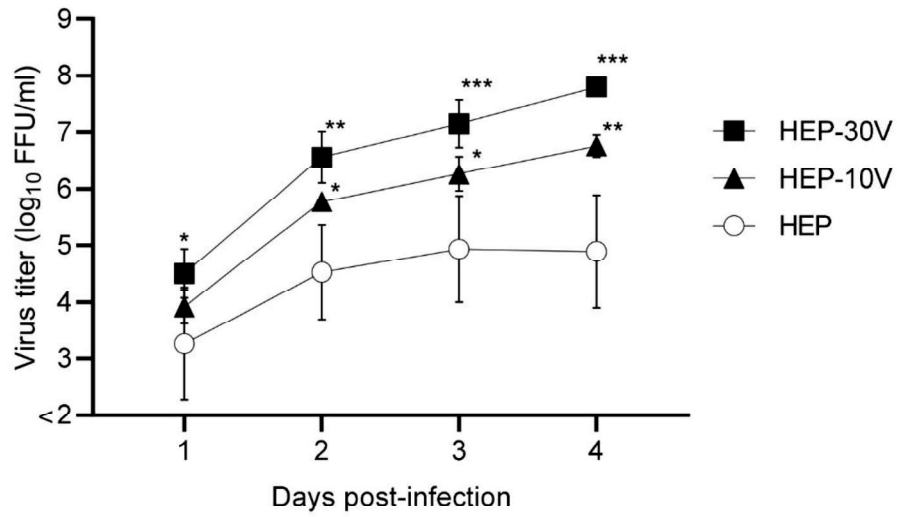
Fig. 8. Viral growth in Vero cells of recombinant HEP with 5 amino acid substitutions identified in Vero-adapted strains, named rHEP-PG4

(a) Information on recombinant viruses used in this figure. *: Amino acid sequence identical with rHEP. **: Amino acid positions are numbered based on the mature G protein without signal peptide. (b) Vero cells were inoculated with the recombinant strains at an M.O.I. of 0.05. Viral titers were determined in MNA cells. The means and S.D. of the log₁₀ of the viral titer calculated from three independent experiments. Significant differences are indicated in the comparison between rHEP-30V and each strain after application of two-way ANOVA followed by Tukey (**: $p < 0.01$, ***: $p < 0.001$). rHEP-30V vs rHEP-10V+G3, rHEP-PG4 had no significant difference at all time points after application of two-way ANOVA followed by Tukey ($p > 0.05$). (c) Virus-neutralizing antibody (VNA) titers were determined by RFFITs using rabbit serum and quantified using IU/ml. Means and S.D. were calculated from three

independent experiments. No significant difference is indicated ($p>0.05$) in the neutralizing activities against rHEP and rHEP-PG4 after application of two-way ANOVA followed by Tukey.

2.7 Figures and tables

(a)



(b)

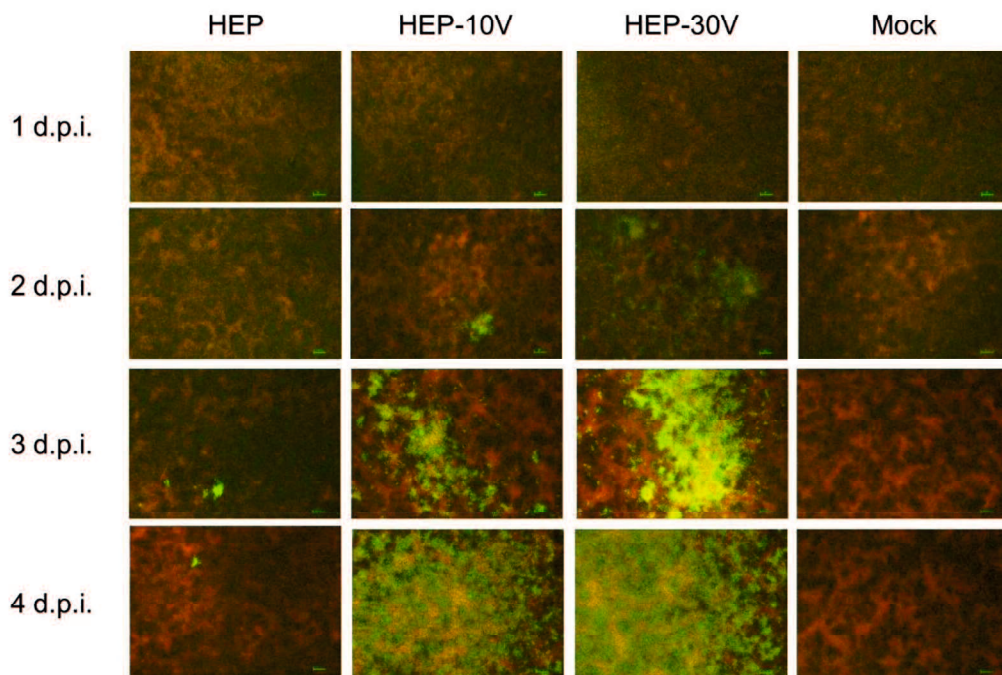


Fig. 1. Viral growth and spread of HEP-Flury (HEP) and Vero-adapted viruses (HEP-10V and -30V) in Vero cells

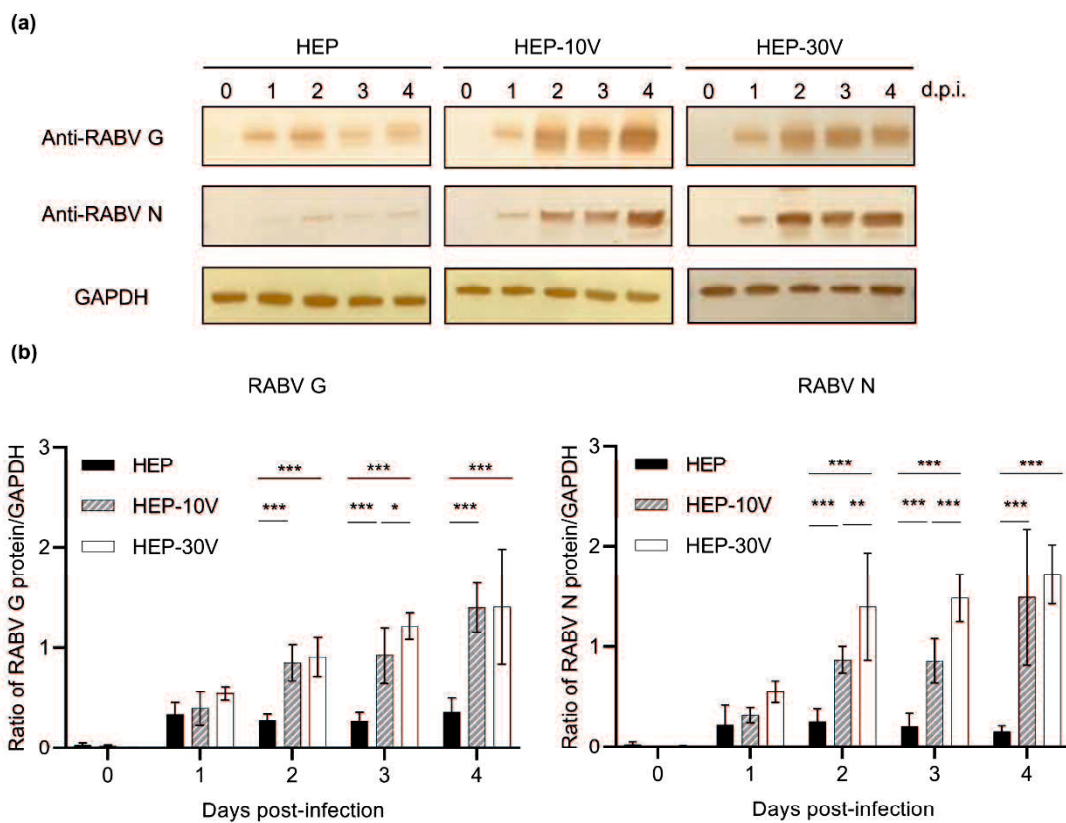


Fig. 2. Comparison of expression of viral proteins among HEP, HEP-10V and HEP-30V in Vero cells

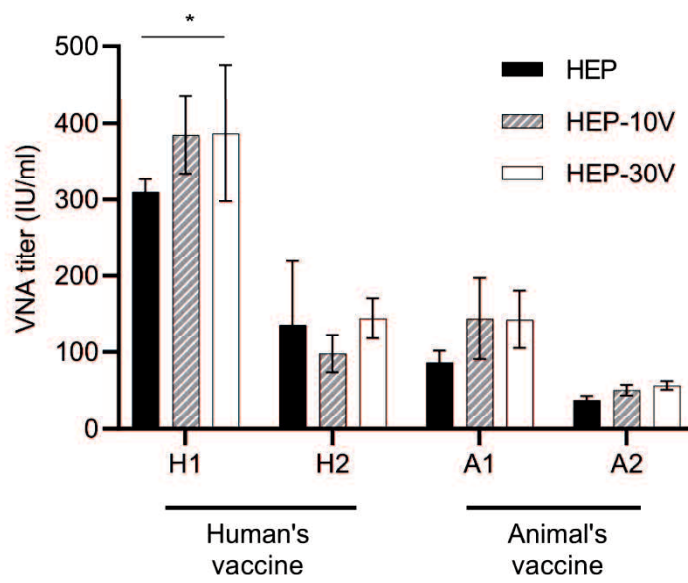


Fig. 3. Comparison of virus-neutralizing antibody titers against HEP, HEP-10V and HEP-30V using vaccinated rabbit sera

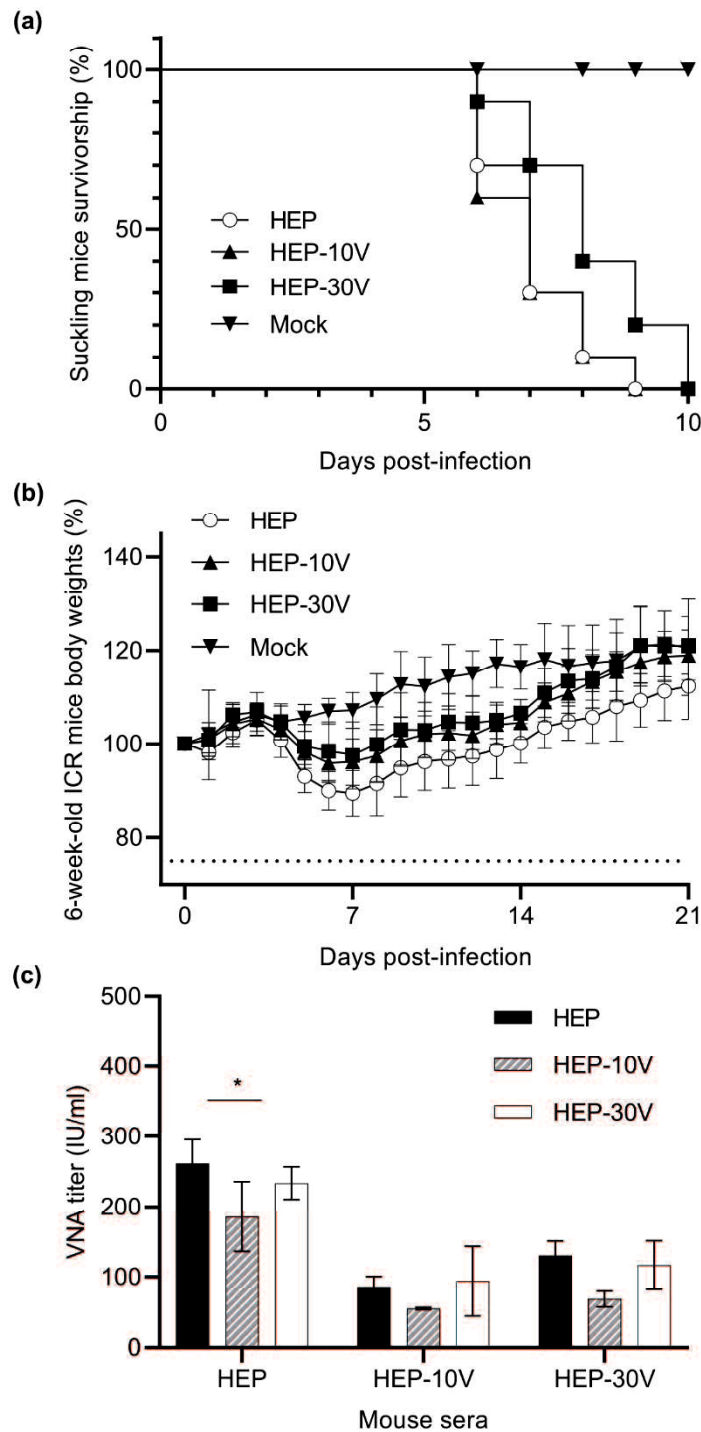


Fig. 4. Comparison of pathogenicity among HEP, HEP-10V and HEP-30V in suckling and 6-week-old mice, and VNA titers against HEP-Flury using sera pooled from each infected-adult mice group

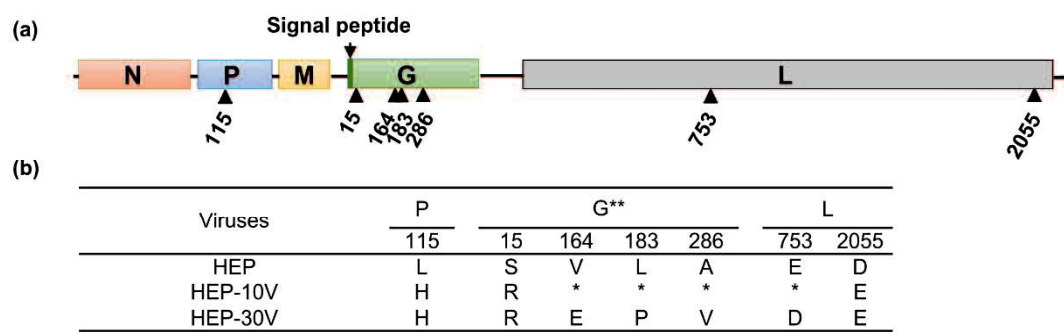


Fig. 5. Comparison of amino acid sequences between HEP, Vero-adapted viruses

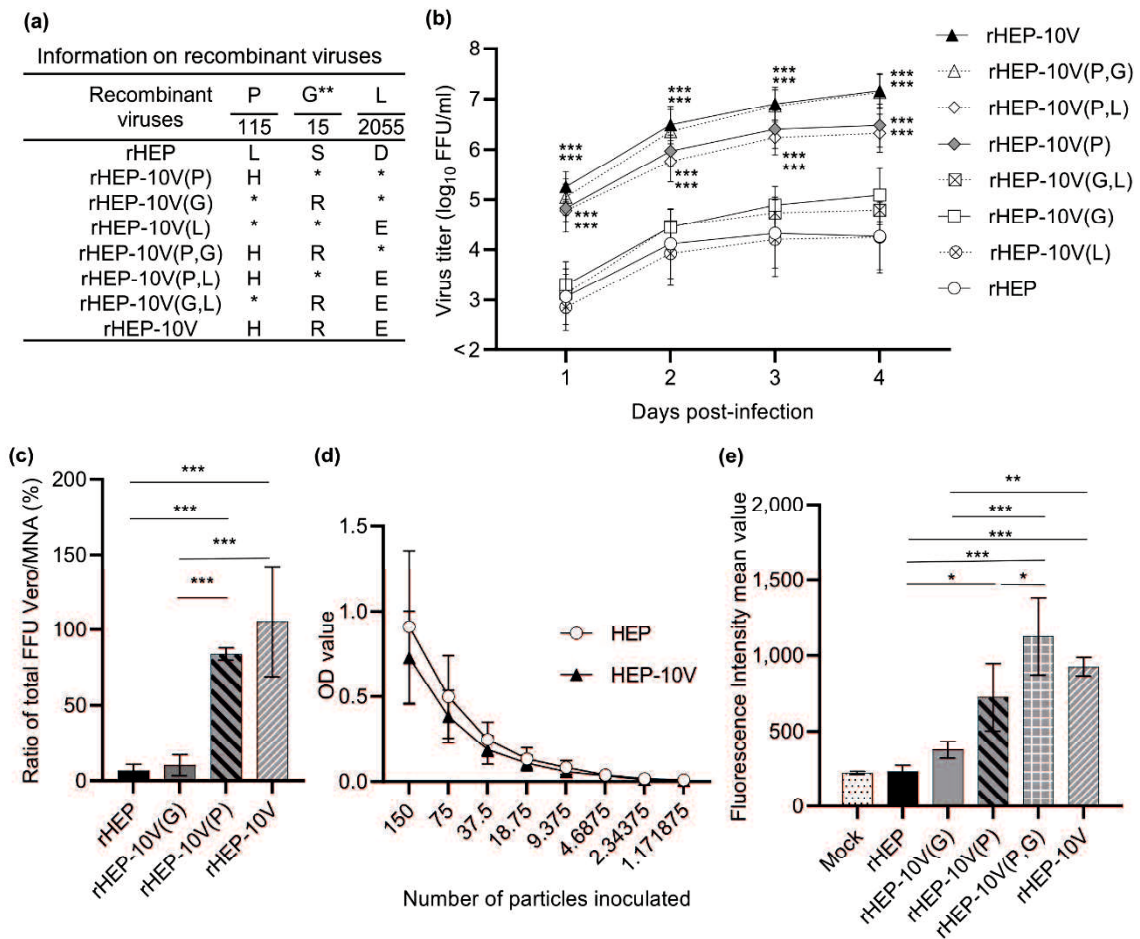


Fig. 6. Efficiency of viral growth, entry, and expression of G protein of each recombinant viruses in Vero cells

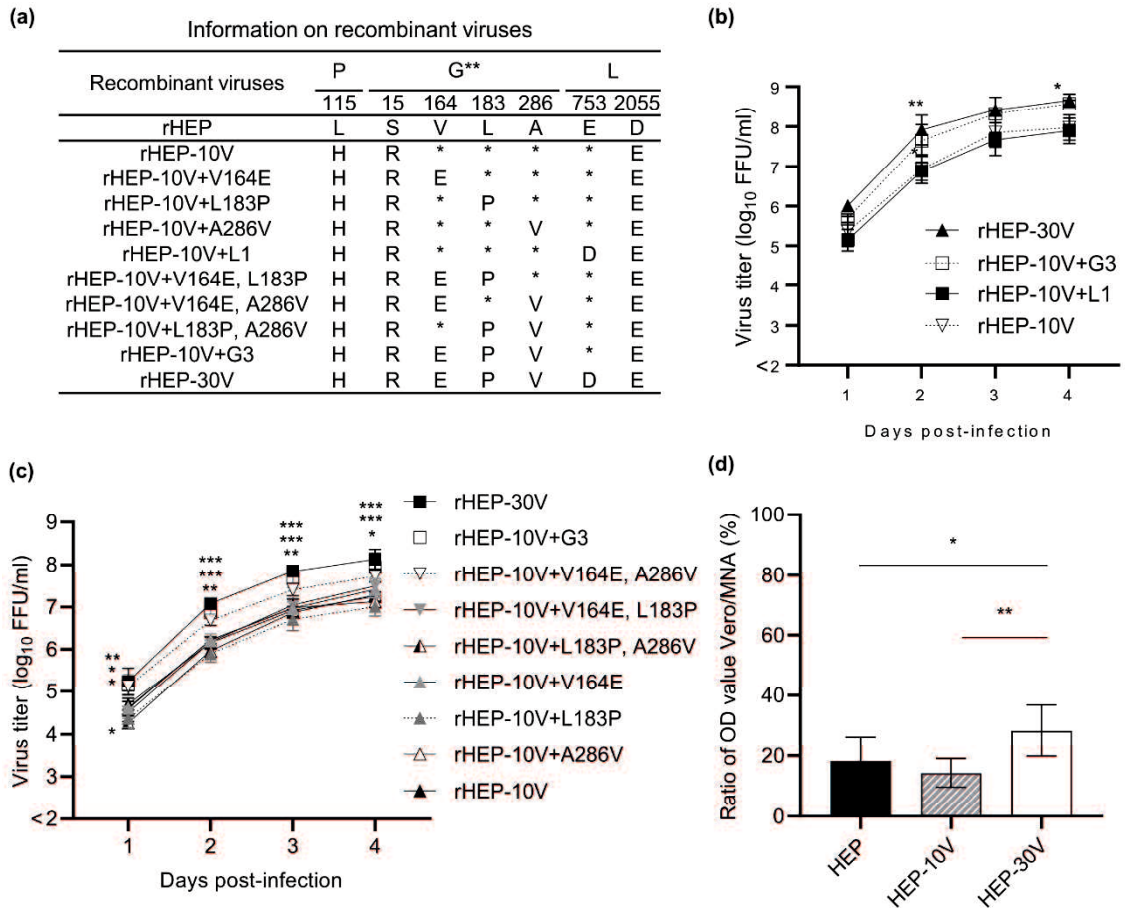


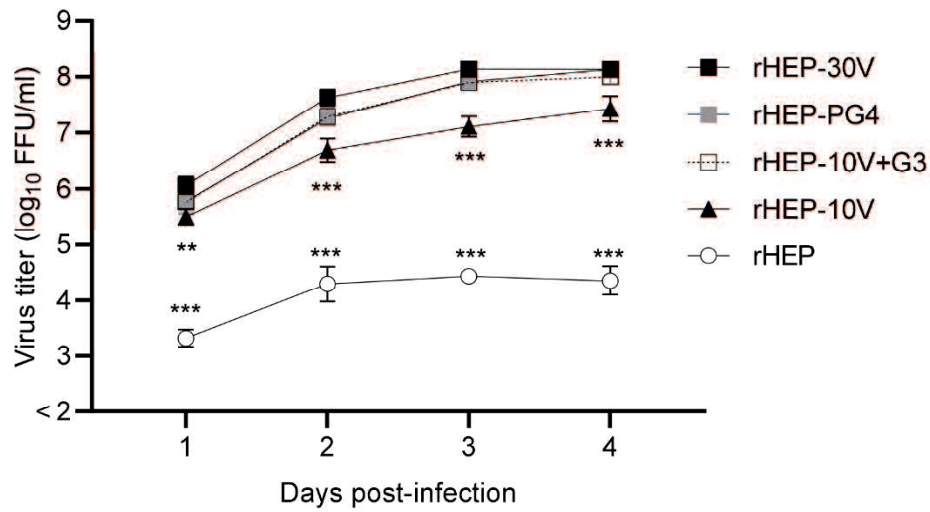
Fig. 7. Comparison of viral growth in Vero cells among recombinant HEP strains, and entry of VSVp pseudotyped with the G protein of HEP, HEP-10V or HEP-30V

(a)

Information on recombinant viruses

Recombinant viruses	P	G**				L	
	115	15	164	183	286	753	2055
rHEP	L	S	V	L	A	E	D
rHEP-10V	H	R	*	*	*	*	E
rHEP-10V+G3	H	R	E	P	V	*	E
rHEP-30V	H	R	E	P	V	D	E
rHEP-PG4	H	R	E	P	V	*	*

(b)



(c)

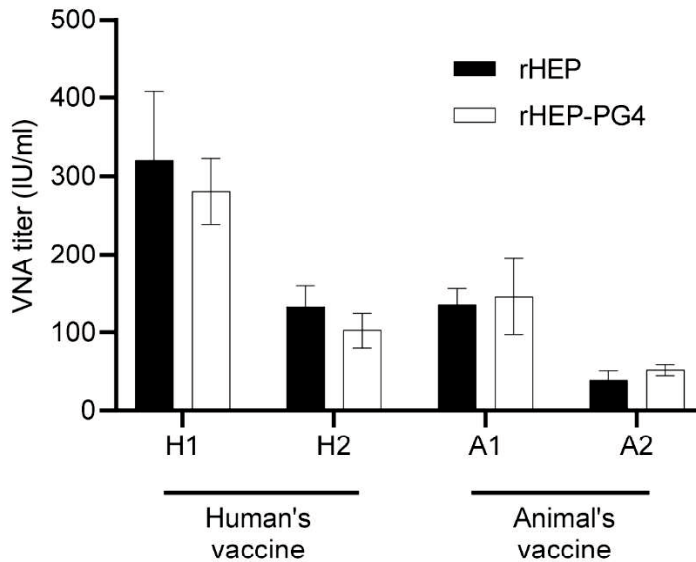


Fig. 8. Viral growth in Vero cells of recombinant HEP with 5 amino acid substitutions

identified in Vero-adapted strains, named rHEP-PG4

2.8 Supplementary Table

Supplementary Table S1. Comparison of amino acid sequences between our laboratory's HEP-Flury (HEP) strain and those previously reported for HEP-Flury strains

Strain	P					M			G (signal peptide) G**											L							
	28	130	191	289	295	16	106	172	14	15	40	120	164	206	236	259	273	484	504	75	383	745	1319	1653	1848	2091	
HEP (LC785439)	I	S	G	D	T	T	A	D	F	P	G	H	V	T	M	N	E	P	R	D	L	Q	R	V	R	R	
AB085828	*	*	*	*	*	*	*	*	S	*	*	*	*	*	*	*	*	*	*	*	*	*	*	*	*	*	*
LC717409	*	T	E	*	*	*	*	N	*	*	*	*	*	*	*	*	V	T	*	*	*	*	*	*	*	*	
GU565704	*	T	E	*	K	*	V	N	*	S	*	*	*	*	*	*	V	T	*	G	S	*	*	*	*	S	
LC717410	*	T	E	*	*	*	V	N	*	*	*	*	*	I	*	*	V	T	I	*	S	*	*	*	*	*	
LC717411	V	T	E	*	*	*	V	N	*	*	*	*	E	I	V	D	V	T	I	*	S	*	K	I	*	*	
LC717412	V	T	E	N	*	I	V	N	*	*	R	V	E	I	V	D	V	T	I	*	S	R	K	*	K	*	

*: Amino acid identical with our laboratory HEP.

** : Position of amino acids in the mature G protein without the signal peptide.

Supplemental Table S2. Comparison of virus titers between HEP-Flury (HEP) and Vero-adapted HEP-Flury strains

Days post infection	Virus titers (\log_{10} FFU/ml) (Mean \pm S.D.)		
	HEP	HEP-10V	HEP-30V
1	3.15 \pm 0.99	3.91 \pm 0.29	4.48 \pm 0.42
2	4.47 \pm 0.83	5.76 \pm 0.11	6.54 \pm 0.45
3	4.87 \pm 0.93	6.25 \pm 0.30	7.14 \pm 0.41
4	4.82 \pm 0.99	6.75 \pm 0.19	7.79 \pm 0.07

Supplemental Table S3. Comparison of virus titers among recombinant HEP-Flury strains to evaluate the effect of mutations in HEP-10V

Days post infection	Virus titers (\log_{10} FFU/ml) (Mean \pm S.D.)							
	rHEP	rHEP-10V(P)	rHEP-10V(G)	rHEP-10V(L)	rHEP-10V(P,G)	rHEP-10V(P,L)	rHEP-10V(G,L)	rHEP-10V
1	3.03 \pm 0.55	4.81 \pm 0.48	3.28 \pm 0.45	2.83 \pm 0.46	5.04 \pm 0.36	4.77 \pm 0.21	3.10 \pm 0.39	5.25 \pm 0.30
2	4.08 \pm 0.68	5.96 \pm 0.31	4.43 \pm 0.35	3.89 \pm 0.63	6.35 \pm 0.43	5.75 \pm 0.40	4.45 \pm 0.36	6.47 \pm 0.36
3	4.28 \pm 0.67	6.39 \pm 0.37	4.88 \pm 0.36	4.16 \pm 0.72	6.85 \pm 0.32	6.23 \pm 0.34	4.73 \pm 0.31	6.90 \pm 0.32
4	4.23 \pm 0.64	6.47 \pm 0.42	5.07 \pm 0.53	4.21 \pm 0.70	7.13 \pm 0.34	6.31 \pm 0.36	4.78 \pm 0.29	7.16 \pm 0.33

Supplemental Table S4. Comparison of virus titers of the rHEP-10V to evaluate the effect of mutations on the G or L proteins in rHEP-30V

Days post infection	Virus titers (\log_{10} FFU/ml) (Mean \pm S.D.)			
	rHEP-10V	rHEP-10V+G3	rHEP-10V+L1	rHEP-30V
1	5.35 \pm 0.37	5.69 \pm 0.10	5.13 \pm 0.26	6.00 \pm 0.09
2	6.92 \pm 0.36	7.64 \pm 0.39	6.87 \pm 0.23	7.90 \pm 0.37
3	7.83 \pm 0.57	8.31 \pm 0.06	7.66 \pm 0.18	8.40 \pm 0.32
4	7.96 \pm 0.31	8.57 \pm 0.09	7.88 \pm 0.31	8.65 \pm 0.16

Supplemental Table S5. Comparison of virus titers among rHEP-10 with the substitutions in rHEV-30V

Days post infection	Virus titers (log ₁₀ FFU/ml) (Mean±S.D.)								
	rHEP-10V	rHEP-10V+V164E	rHEP-10V+L183P	rHEP-10V+A286V	rHEP-10V+V164E, L183P	rHEP-10V+V164E, A286V	rHEP-10V+L183P, A286V	rHEP-10V+G3	rHEP-30V
1	4.69±0.13	4.61±0.05	4.35±0.20	4.58±0.17	4.5±0.14	5.12±0.10	4.26±0.03	5.14±0.25	5.23±0.31
2	6.14±0.14	6.21±0.15	5.89±0.19	6.21±0.08	6.16±0.04	6.68±0.11	5.96±0.15	6.86±0.08	7.08±0.08
3	6.91±0.09	6.96±0.14	6.70±0.27	6.97±0.20	7.04±0.19	7.40±0.14	6.86±0.05	7.68±0.22	7.84±0.05
4	7.24±0.10	7.41±0.20	7.00±0.21	7.13±0.14	7.49±0.17	7.72±0.13	7.28±0.06	7.93±0.11	8.13±0.23

Supplemental Table S6. Comparison of virus titers of the rHEP-PG4 with only five substitutions

Days post infection	Virus titers (\log_{10} FFU/ml) (Mean \pm S.D.)				
	rHEP	rHEP-10V	rHEP-10V+G3	rHEP-PG4	rHEP-30V
1	3.31 \pm 0.15	5.50 \pm 0.14	5.75 \pm 0.18	5.77 \pm 0.22	6.06 \pm 0.15
2	4.28 \pm 0.31	6.69 \pm 0.20	7.28 \pm 0.16	7.25 \pm 0.05	7.62 \pm 0.14
3	4.43 \pm 0.08	7.10 \pm 0.17	7.89 \pm 0.10	7.91 \pm 0.10	8.13 \pm 0.08
4	4.35 \pm 0.25	7.42 \pm 0.22	7.99 \pm 0.12	8.12 \pm 0.11	8.12 \pm 0.03

Supplementary Table S7. Primers used for sequence analysis.

Primer	Forward primer (5'-3')	Position*	Reverse primer (5'-3')	Position*
RABV1	ACAGACAGCGTCAATTGCAAAGC	28–50	TTGACGAAGATCTTGCTCAT	1533–1514
RABV2	CTTCCGTTCACTAGGCTTGAGTGGG	934–958	GGRGGTGAAGCCACARGTCATCG	2602–2579
RABV3	TGATCTATCAGTRGAGGCTGAGATCGC	2092–2118	CTGAAGAGACATGTCAGACCATAG	3056–3033
RABV4	ATGRCGATGACYTGTGGCTCCACC	2575–2599	CCCATGTTCCATCCATAAGTCTAAG	4095–4071
RABV5	TATCCCGCAAGTTCATCACT	3113–3132	AGTTTGGCAGAGTCCTCAATC	5556–5536
RABV6	GGGTTTGAAAAGCATATACCATATTC	4302–4328	GACTTGAATAGAAATGGGCCAAGTC	5790–5765
RABV7	TGTCCCAACATCTTGAGGAACTC	5488–5510	CGCATTGGTGGATACTGTAGA	7912–7892
RABV8	TACTAGCTCAAGGAGACAACCAGGT	7581–7605	TGAACCAGTTTATAGATTCTTTAACG	9017–8991
RABV9	TCAGAGTTTCGAGAGGCAATCCTG	8399–8422	AGCTGCATGGCGCACCTCTTGATC	10249–10226
RABV10	CAGCTCAGGGGCTCTTATACTCAATC	9555–9580	CCAGAGGTTCCGATTCAAGA	11880–11861

*: The positions of the primer locations were defined based on the newly amplified genomic sequence of HEP using these primer sets.

Supplementary Table S8. Primers used for construction of infectious clones.

Primer	Forward primer (5'–3')	Position*	Reverse primer (5'–3')	Position*
Full-genome1	ACGCTTAACAACAAAACCAAAGAAG	1–25	TGAGCGATCTCAGCCTCYACTGATAG	2121–2096
Full-genome2	CTCCGTTCACTAGGCTTGAGTGGG	934–958	GGACCAAGTTTGTCTGGTATCG	3412–3391
Full-genome3	CTATGGTCTGACATGTCTCTTCAG	3033–3056	GACTTGGAAATAGAAATGGGCCAAGT C	5790–5765
Full-genome4	TGTCCCAACATCTTGAGGAACTC	5488–5511	CGCATTGGTGGATACTGTAGA	7912–7892
Full-genome5	TACTAGCTCAAGGAGACAACCAGGT	7581–7605	AGCTGCATGGCGCACCTCTTGATC	10249–10226
Full-genome6	CAGCTCAGGGGCTCTTATACTCAATC	9555–9580	ACGCTTAACAATAAAACAATAAAGAT	11925–11900
Kpn_HamRz_HEP	<u>ATAGGTACCTGTTAAGCGTCTGATGA</u> <u>GTCCGTGAGGACGAACTATAGGAA</u> <u>AGGAATTCCTATAGTCACGCTTAACA</u> ACAAAACCAAAGAAGAAGCA*	1–30	<u>CGGCTGCAGCGCCCTCCCTTAGCCAT</u> <u>CCGAGTGGACGTGCGTCCTCCTTCG</u> <u>GATGCCCAGGTCGGACCGCGAGGAG</u> <u>GTGGAGATGCCATGCCGACCCACGC</u> TTAACAAATAACAATA*	11925–11905
Pst_HdvRz_HEP				

Note that ribozyme sequences are underlined.

*: The positions of the primer locations were defined based on the newly amplified genomic sequence of HEP using these primer sets.

Supplementary Table S9. Primers used for construction of helper plasmids

Primer	Forward primer (5'-3')	Position*	Reverse primer (5'-3')	Position*
helper N	ATAGGTACCATGGATGCCGACAAG	67–85	CGGCTGCAGTTATGAGTCACTCG	1423–1410
helper P	ATAGGTACCATGAGCAAGATCTTTG	1511–1529	CGGCTGCAGTTAGCATGATGTGTAG	2408–2392
helper G	ATAGGTACCATGGTTCCTCAGGTTC	3318–3333	CGGCTGCAGTCACAGTCTGGTCTCG	4892–4877
helper L	ATAGGTACCATGCTGGATCCGGGA	5411–5425	CGGCTGCAGTTACAAACAACGTAG	11794–11779

*: The positions of the primer locations were defined based on the newly amplified genomic sequence of HEP using these primer sets.

Supplemental Table 10. Primers used for construction of recombinant viruses.

Primer	Forward primer (5'-3')	Position*	Reverse primer (5'-3')	Position*
HEP-10V_P_L115H	AGATTCCACAAGATATGGTCACAG ACCGTAGAG	1850–1882	TATCTTGTGGAATCTCTCCTGACCT CATTG	1864–1832
HEP-10V_G_S15R	CCCTGGAGACCTATTGACTTACACC ATCTCAGC	3411–3443	AATAGGTCTCCAGGGACCAAGTTTGT CTGGTAT	3425–3393
HEP-10V_L_L2055E	TGGTCCGAGGACACCCCAGTGTTT AAGAGGGTA	11567–11599	GGTGTCTCCGGACCAGCTCCAAGATA GATAGAT	11581–11549
HEP-30V_L_E753D	GAGTTAGATAGCATATCGAGGAAT GCACTCTCA	7661–7693	TATGCTATCTAACTCATAGAGAAGCC CCTCTTG	7675–7643
HEP-30V_G_V164E	ATAACGGAGTCCTCGACCTACTGC TCAACTAA	3858–3889	CGAGGACTCCGTTATTCCTGAGCAAT TTCCGCC	3872–3840
HEP-30V_G_L183P	GAGAATCCGAGACTAGGGACATCT TGTGACATT	3915–3947	TAGTCTCGGATTCTCAGGCATCCAGA TGGTGTA	3929–3897
HEP-30V_G_A286V	CTGGATGTACTAGAGTCCATCATG ACCACCAAG	4224–4256	CTCTAGTACATCCAGACACTCCTCTC TTTTCTTG	4238–4205

*: The positions of the primer locations were defined based on the newly amplified genomic sequence of HEP using these primer sets.

3. Chapter 2: Single amino acid substitution in the matrix protein of rabies virus is associated with neurovirulence in mice.

3.1 Abstract

Rabies is a fatal encephalitic infectious disease caused by the rabies virus (RABV). RABV is highly neurotropic and replicates in neuronal cell lines *in vitro*. The RABV fixed strain, HEP-Flury, was produced via passaging in primary chicken embryonic fibroblast cells. HEP-Flury showed rapid adaptation when propagated in mouse neuroblastoma (MNA) cells. In this study, we compared the growth of our previously constructed recombinant HEP (rHEP) strain—based on the sequence of the HEP (HEP-Flury) strain—with that of the original HEP strain. The original HEP strain exhibited higher titer than rHEP and a single substitution at position 80 in the matrix (M) protein M(D80N) after incubation in MNA cells, which was absent in rHEP. *In vivo*, intracerebral inoculation of the rHEP-M(D80N) strain with this substitution resulted in enhanced viral growth in the mouse brain and a significant loss of body weight in the adult mice. The number of viral antigen-positive cells in the brains of adult mice inoculated with the rHEP-M(D80N) strain was significantly higher than that with the rHEP strain at 5 days post-inoculation. Our findings demonstrate that a single amino acid substitution in the M protein M(D80N) is associated with neurovirulence in mice owing to adaptation to mouse neuronal cells.

3.2 Introduction

Rabies is a lethal zoonotic disease, which causes encephalitis in almost all mammalian species¹. An estimated 59,000 rabies cases are reported worldwide annually², and over 99% of human rabies cases are transmitted from dogs . The World Health Organization (WHO) is promoting “the global strategic plan to end human deaths from dog-mediated rabies by 2030: Zero by 30”^{5,7}.

Rabies is caused by rabies virus (RABV) infection. RABV is a non-segmented, single negative-stranded RNA virus belonging to the *Lyssavirus* genus of the *Rhabdoviridae* family. The viral genome encodes five structural proteins: the nucleoprotein (N protein), phosphoprotein (P protein), matrix (M) protein, glycoprotein (G protein), and large RNA-dependent RNA polymerase (L protein). After infection, RABV shows high neurotropism^{10,28}, resulting in its migration from the peripheral nervous system to the central nervous system^{73,74}. RABV can easily replicate in neurological cell lines, such as mouse neuroblastoma (MNA) cells^{75,76}, mouse neuroblastoma (N2a) cells⁷⁷, and human neuroblastoma (SK-N-SH) cells⁷⁸. To produce attenuated strains, street strains isolated from animals have been serially passaged into neuronal cells⁶⁴, baby hamster kidney fibroblasts (BHK cells)^{79,80}, and suckling mice⁸¹, showing multiple substitutions. Major changes occur in the G protein after passage, and it is associated with multiple functions,

including pathogenicity, antigenicity, and cell entry. Position 333 in the G protein is associated with pathogenicity and leads to changes in the mortality of infected mice^{26,28,29}. The relationship of the M protein with pathogenicity and neurovirulence is not known in detail but it has been reported that the position 95 in this protein affects viral pathogenicity in mice⁸².

The Flury strain of RABV isolated from a girl who died of rabies was transferred to 1-day-old chicks in 1940⁶. Subsequently, the Flury strain was passaged over 180 times in chicken eggs to generate the high-egg-passage Flury strain (HEP-Flury)^{6,25-27}. HEP-Flury was propagated in primary chicken embryo fibroblast cells for use as a human rabies vaccine strain⁶, and a chick embryo cell-adapted HEP-Flury small plaque-forming (CEF-S) strain was produced²⁵. After intracerebral inoculation, HEP-Flury was highly attenuated. It is lethal in suckling mice and not adult mice²⁸. The HEP-Flury strain can replicate, yielding high titers in MNA cells similar to other RABV strains^{10,28}.

In this study, our previously constructed recombinant HEP (rHEP) strain, based on the sequence of the HEP (HEP-Flury) strain from our laboratory, was characterized. We compared the propagation of the two strains in MNA cells. Infection with the original HEP strain produced significantly higher titers than rHEP strain despite the same sequence. Furthermore, we found a single substitution in the M protein between rHEP

and the virus recovered from MNA cells infected with HEP. We characterized a single substitution in the M protein, M(D80N), and analyzed the virus propagation in MNA cells and its virulence in a mouse model. The results suggested that one substitution in the M protein play a crucial role in neuropathogenesis of RABV.

3.3 Materials and Methods

3.3.1 Cells and Viruses

MNA and BHK-21 cells were grown at 37 °C in Eagle's minimum essential medium (MEM) (Nacalai Tesque, Kyoto, Japan) supplemented with 10% heat-inactivated fetal bovine serum (FBS) (Gibco, Grand Island, NY, USA). Chicken embryo fibroblast cells (DF-1) (CRL-12203; American Type Culture Collection (ATCC), Manassas, VA, USA) were maintained at 39 °C in Dulbecco's modified Eagle's minimum essential medium (DMEM) (Nacalai Tesque) supplemented with 10% heat-inactivated FBS.

The RABV used in this study was a laboratory strain of HEP-Flury (HEP) (Accession Number: LC785439), which was originally stocked in our laboratory after two rounds of propagation in MNA cells. Cloned HEP (cHEP) and cHEP-M(D80N) were cloned following the limiting dilution method using the supernatant of HEP-infected MNA cells at 2 d.p.i.

3.3.2 Reverse transcription-polymerase chain reaction (RT-PCR)

RABV RNA was extracted from the supernatant of infected cells using the QIAamp Viral RNA Mini Kit (QIAGEN, Hilden, Germany) according to the manufacturer's protocol. To generate cDNA, reverse transcription was performed as previously described⁵³, and this cDNA was used for subsequent PCR amplification of RABV

genome fragments. The cDNA templates were subjected to PCR using Prime STAR GXL (TaKaRa Bio, Shiga, Japan) and the respective primer sets (Supplementary Table S1). Purified PCR products were analyzed using the Sanger sequencing method. Sequence assembly and further analysis were conducted using GENETYX Ver.15 software (GENETYX, Tokyo, Japan) and Sequence Scanner (Thermo Fisher Scientific, Waltham, MA, USA).

3.3.3 Constructing and rescuing recombinant RABVs

To construct an infectious clone of RABV, PCR was performed using Prime STAR GXL (TaKaRa Bio), followed by Phusion Hot Start II High-Fidelity DNA Polymerase (Thermo Fisher Scientific) for the entire RABV genome. Mutant viruses were constructed by introducing point mutations through PCR using Prime STAR Max (TaKaRa Bio) and synthetic primers (Supplementary Table S1) with the indicated sequences. The assembled cDNA of the full RABV genome flanked by the hammerhead and delta virus ribozymes sequences (HamRz and HdvRz, respectively) was inserted between the KpnI and PstI sites of the pcDNA3.1 Zeo (+) plasmid (Thermo Fisher Scientific), as previously reported⁵⁴. To construct helper plasmids, genes encoding N, P, G, and L proteins were amplified from HEP using conventional PCR (Supplementary Table S2) and cloned

between the KpnI and PstI sites of the same vector.

BHK-21 cells (3.0×10^5 cells/well) were grown overnight in six-well plates and transfected with 1.2 μg of the full-length plasmid and 450 ng each of helper plasmids. Transfection was conducted using the TransIT-LT1 Transfection Reagent (Mirus Bio, Madison, WI, USA) following the manufacturer's protocol. After five days, the supernatants were collected, and an aliquot was used for inoculation into MNA cells to confirm the presence of the virus using a direct fluorescent antibody test (DFAT). Supernatants from virus-positive wells (confirmed by DFAT) were propagated only once in MNA cells to obtain a virus stock. The nucleotide sequences of all rescued viruses were confirmed through sequencing.

3.3.4 Virus titration

MNA cells were seeded (4.0×10^4 cells/well) in 96-well plates and incubated overnight at 37 °C with 5% CO₂. Subsequently, serial 10-fold dilutions of the virus or the 10% brain emulsion in phosphate-buffered saline (PBS) were inoculated into the cells, which were then incubated at 37 °C for 2 days. The cells were fixed with 80% acetone for 30 min and stained with fluorescein isothiocyanate (FITC) anti-rabies monoclonal globulin (FUJIREBIO, Tokyo, Japan). Antigen-positive foci were counted under a

fluorescence microscope (Nikon, Tokyo, Japan) and quantified in focus-forming units (FFU) per milliliter.

3.3.5 Comparing viral growth

MNA and DF-1 cells in 6-well plates were inoculated with each RABV strain at a multiplicity of infection (M.O.I.) of 0.05. After 1 h of adsorption, the cells were washed three times with MEM or DMEM, and 2 mL of MEM or DMEM supplemented with 10% heat-inactivated FBS was added to each well. The supernatant was collected at the indicated time points. Each experiment was independently repeated two or three times.

3.3.6 Animal experiments

The animal study protocol was approved by the Committee for Animal Experimentation at our institute (NIID) (Approval Number: 123129). All possible efforts were made to minimize the suffering of laboratory animals. The mice were housed in the animal facility of the NIID. Six-week-old ICR (adult) mice (5/group) or suckling mice (10/group) (Japan SLC, Shizuoka, Japan) were inoculated intracerebrally with 10^5 FFU/mouse of rHEP, rHEP-M(D80N), or MEM (as a negative control “mock”). The body weights of adult mice were monitored until 20 d.p.i., and mortality was recorded daily at

10 d.p.i. for suckling mice. The brains of the suckling mice were collected after death or euthanasia. Additionally, six-week-old ICR (adult) mice (3/group) were intracerebrally inoculated with 10^5 FFU/mouse of the recombinant strains, and brain samples were collected at 5 and 7 d.p.i. for DFAT and virus titration. Brain samples from suckling mice (10/group) and adult mice (3/group) were applied with a toothpick to a 3-well microslide glass (Matsunami, Osaka, Japan), and each well was air-dried. Slides were fixed in 10% formalin supplemented with 0.4% TritonX-100 (Merck, Darmstadt, Germany) for 1 h and stained with FITC Anti-Rabies Monoclonal Globulin. The cells were counterstained with Evans Blue (FUJIFILM Wako Pure Chemical Corporation, Osaka, Japan).

3.3.7 Statistical analysis

Data are presented as mean \pm standard deviation (S.D.). Statistical analyses were conducted using the two-way analysis of variance (ANOVA), followed by Tukey's or Sidak's multiple-comparison tests. Unpaired *t*-tests were two-tailed. The log-rank test was used to analyze the Kaplan–Meier survival curves. Statistical analyses were performed using GraphPad Prism 9 (GraphPad Software, San Diego, CA, USA). Values of $p < 0.05$ were considered statistically significant.

3.4 Results

3.4.1 Comparison of viral growth between original and recombinant HEP

Recombinant HEP (rHEP) was obtained via transfection of BHK-21 cells with the full-length plasmid and four helper plasmids encoding N, P, G, and L proteins. Supernatants were propagated only once in MNA cells to obtain a virus stock, and the nucleotide sequence of rHEP was confirmed to be identical to that of the original HEP (DDBJ Accession No. LC785439). A significant difference was observed between original HEP and rHEP, when we compared their viral growth in MNA cells at an M.O.I. of 0.05 (Fig. 1a), resulting in the original HEP growing significantly more in MNA cells at 1–3 d.p.i. than rHEP. We verified that the sequences of original HEP and rHEP were identical via Sanger sequencing, and then, we compared the nucleotide sequences of HEP collected from the supernatant at 2 d.p.i. The results revealed a single mixture of nucleotide sequences at position 238 (guanine and adenine) in the M gene of the HEP strain, resulting in a mixture of aspartic acid (D) and asparagine (N) at position 80 in the M protein (Fig. 1b). In contrast, rHEP showed no change in amino acid content. Subsequently, we examined the sequences of HEP after serial passages in MNA cells, which resulted in an increase in the substitution from guanine to adenine at position 238 (Supplementary Figure S1). As HEP was highly passaged in chicken embryo cells, the viral growth of

HEP and rHEP in DF-1 was compared. There were no significant differences in viral growth between HEP and rHEP (Figure 1f). Furthermore, there was no change in the HEP nucleotide sequence after propagation in DF-1 cells (Supplementary Figure S2).

3.4.2 Comparing viral growth of limiting dilution viruses

After the propagation of HEP in MNA cells, the viral solution contained a mutant with a substitution of M(D80N). cHEP and cHEP-M(D80N) were cloned via limiting dilution from the supernatant collected at 2 d.p.i. Nucleotide sequence analysis confirmed only one substitution among the cloned viruses (Fig. 1d). cHEP and cHEP-M(D80N) strains were inoculated into MNA cells, and their viral growth was compared (Fig. 1c). The cHEP-M(D80N) grew significantly better than cHEP.

3.4.3 Comparison of viral growth of recombinant HEP-M(D80N)

To confirm the enhancement in viral growth caused by the single substitution in the M protein, M(D80N), the recombinant HEP-M(D80N) strain, rHEP-M(D80N), was constructed using reverse genetics, and the viral growth of rHEP-M(D80N) was compared with that of rHEP. rHEP-M(D80N) grew significantly better in MNA cells than rHEP (Fig. 1e) but not in DF-1 cells (Fig. 1f). These results indicate that only one

substitution of M(D80N) enhanced viral growth in MNA cells.

3.4.4 Pathogenicity of recombinant HEP-M(D80N)

To compare the pathogenicity of rHEP and rHEP-M(D80N), 105 FFU of each virus was inoculated intracerebrally into suckling ICR mice (Fig. 2a) and 6-week-old adult ICR mice (Fig. 2b). Suckling mice infected with rHEP or rHEP-M(D80N) showed neurological signs at 4 d.p.i. and subsequently died at 5–8 d.p.i. (Fig. 2a). For both strains, all infected adult mice survived until 20 d.p.i. and showed no clinical signs other than body weight loss (Fig. 2b). These inoculated adult mice exhibited loss of body weight at 4 d.p.i and recovered from 7 d.p.i. Notably, mice inoculated with rHEP-M(D80N) showed a more significant body weight loss than those inoculated with rHEP.

A DFAT was performed using RABV nucleoprotein monoclonal antibody to compare viral antigens in the brain. The number of fluorescence-positive cells in the brains of suckling mice inoculated with rHEP-M(D80N) was significantly higher than that in those inoculated with rHEP (Fig. 2c and Supplementary Figure S3). Additionally, the virus titer in mice inoculated with rHEP-M(D80N) was significantly higher than that with rHEP when the 10% brain emulsion was titrated (Fig. 2d). In adult mice, the number of fluorescence-positive cells was higher in the brains inoculated with rHEP-M(D80N) than

in those inoculated with rHEP at 5 d.p.i., during the start of body weight loss (Fig. 2e and Supplementary Figure S4). The titer of the 10% brain emulsion was almost undetectable at 5 and 7 d.p.i. (Fig. 2f), and no positive cells were found in brain samples from either group at 7 d.p.i. (Supplementary Figure S4).

3.5 Discussion

Our findings demonstrate that our laboratory strain (HEP) grew better in MNA cells than rHEP. The nucleotide sequences of HEP collected at 2 d.p.i. indicated a mixture of adenine and guanine in the original HEP at position 238 of the M gene. After the passage of HEP in MNA cells, the proportion of adenine increased, and there was little guanine in the third passage of HEP. This mutation induced a change in the amino acid from aspartic acid (D) to asparagine (N) at position 80 in the M protein. Subsequently, we cloned the viruses cHEP and cHEP-M(D80N) via limiting dilution and constructed recombinant HEP-M(D80N). Viruses with the M(D80N) substitution grew in MNA cells significantly better than those without the substitution, suggesting that this M(D80N) substitution enhanced viral growth in MNA cells. In contrast, there was no significant difference in viral growth in chicken DF-1 cells regardless of the mutation. We hypothesize that the M(D80N) substitution may be important for viral growth in mouse neuronal cells.

Adult mice inoculated with rHEP-M(D80N) showed significantly reduced body weights compared to those inoculated with rHEP, and the number of RABV-positive cells in the rHEP-M(D80N)-infected mouse brain was significantly higher than that in the rHEP-infected mouse brain. Furthermore, the viral titers in the brains of rHEP-M(D80N)-infected suckling mice were significantly higher than those in the brains of rHEP-infected

mice. These results indicate that mutation M(D80N) enhances neurovirulence by enhancing viral growth in the mouse brain.

M protein is crucial in RABV replication and morphogenesis, including viral assembly and budding^{13,83,84}. The late-budding domain of the M protein (amino acid position: 35–38) is related to replication and pathogenicity^{85,86}, and the intermediate filament protein (desmin) interacts with the M protein to regulate viral replication⁸⁷. Additionally, the amino acid at position 95 of the M protein is associated with cell membrane disruption^{82,88}. The RABV M protein is associated with stimulation of the JAK-STAT pathway through its interaction with the P protein and inhibition of the interferon-stimulated response element (ISRE) and IFN- α and IFN- β production⁸⁹, and the amino acids at positions 77, 100, 104, and 110 in the M protein were associated with this pathway^{89,90} resulting in the enhancement in viral replication. Moreover, in RABV strains SN and SB, the exchange of the corresponding M proteins leads to changes in growth in mouse neuroblastoma cells⁹¹. These reports and our results demonstrate that the M protein is critical for viral replication in mouse neuroblastoma cells.

There was no change in the nucleotide sequence of the M gene after the rHEP strain was passaged ten times in MNA cells. Viral sequences from the supernatant on day 4 after the inoculation of DF-1 cells with HEP did not show any change in the M gene

(Supplementary Figure S2). These results suggest that the M(D80N) substitution is important for increased replication in mouse neuronal cells but is not necessary. The rHEP-M(D80N) strain replicated well in the mouse brain, and the number of RABV-positive cells in the brains of mice inoculated with rHEP-M(D80N) was higher at 5 d.p.i. Amino acid substitution M(D80N) is crucial in neurovirulence by enhancing viral growth in neuronal cells. Further studies are required to elucidate the underlying mechanisms. In conclusion, this novel finding demonstrates that the M protein is associated with neurovirulence in mice owing to adaptation to mouse neuronal cells. The amino acid substitution, that is, M(D80N) may play a crucial role in this adaptation.

3.6 Figure legends

Fig. 1. Comparison of viral growth and nucleotide sequences.

Each strain was inoculated into MNA (a, c, e) or DF-1 cells (f) at a multiplicity of infection (M.O.I.) of 0.05. Growth curves of MNA cells were compared between HEP and recombinant HEP (rHEP) (a), cloned HEP (cHEP) and cHEP-M(D80N) (c), and rHEP and rHEP-M(D80N) (e). In DF-1 cells, the growth curves were compared with HEP, rHEP, and rHEP-M(D80N) (f). For viral titration, antigen-positive foci were counted under a fluorescence microscope and calculated as focus-forming units (FFU) per milliliter. The mean viral titer and standard deviation (S.D.) were calculated from two or three independent experiments. Significant differences are indicated (*: $p < 0.05$, **: $p < 0.01$, ***: $p < 0.001$) after two-way analysis of variance (ANOVA) followed by Tukey's test. Nucleotide sequences from the original HEP strain and the supernatant of MNA cells infected with HEP at 2 days post-infection (d.p.i.) (b) and those from cHEP and cHEP-M(D80N) (d) were compared. The sequences of these strains were determined and compared using GENETYX Ver.15 (GENETYX, Tokyo, Japan) and a Sequence Scanner (Thermo Fisher Scientific, Waltham, MA, USA). The arrowhead points to nucleotide position 238 (amino acid position 80) in the M protein. Black, orange, and red arrowheads indicate guanine, adenine, and a mixture of adenine and guanine, respectively. HEP: high-

egg-passage Flury laboratory strain.

Fig. 2. Comparison of pathogenicity between rHEP and rHEP-M(D80N) in suckling and 6-week-old mice.

Suckling (n=10/group) (a, c, d) and 6-week-old mice (n=5/group) (b) were inoculated by intracerebral injection of 10⁵ FFU of the respective virus per mouse, or with an equivalent volume of medium (mock). Plots showing the survival rate of suckling mice using a Kaplan–Meier plot (a) and relative body weights (normalized to baseline) of 6-week-old mice (b). Body weight data are presented as the mean, and error bars represent the S.D. of each group. Significant differences are indicated (*: $p < 0.05$, **: $p < 0.01$) in the relative body weights between rHEP and rHEP-M(D80N) after the application of two-way ANOVA followed by Tukey’s test. The number of RABV-positive cells and viral titers in brain samples from all suckling mice (n=10/group) after death (c,d) and adult mice (n=3/group) at 5 d.p.i. (e) or 5 and 7 d.p.i. (f) were examined. The brain tissue was placed on a slide using toothpick (c, e), fixed in 10% formalin supplemented with 0.4% Triton X-100 solution, stained with fluorescein isothiocyanate (FITC)-conjugated anti-rabies monoclonal globulin (FUJIREBIO, Tokyo, Japan), and examined under a fluorescence microscope. Positive cells were quantified using ImageJ software (National

Institutes of Health, Bethesda, MD, USA). Means and S.D. were calculated from two independent experiments, and significant differences are indicated (**: $p < 0.01$) after application of the unpaired t -test followed by two-tailed tests. For viral titration, a 10% brain emulsion with phosphate-buffered saline (PBS) was prepared (d,f).

3.7 Figures and tables

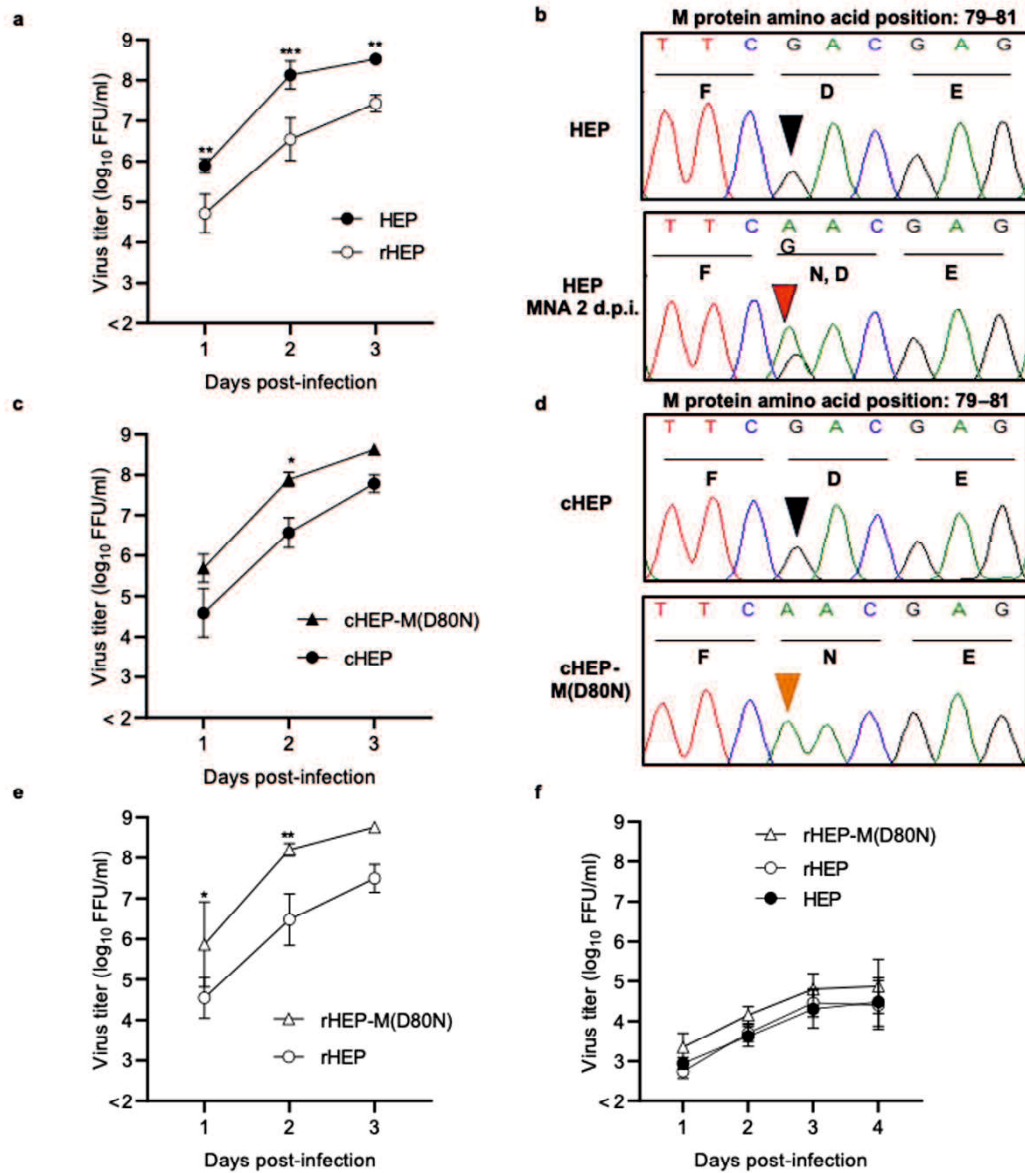


Fig. 1. Comparison of viral growth and nucleotide sequences.

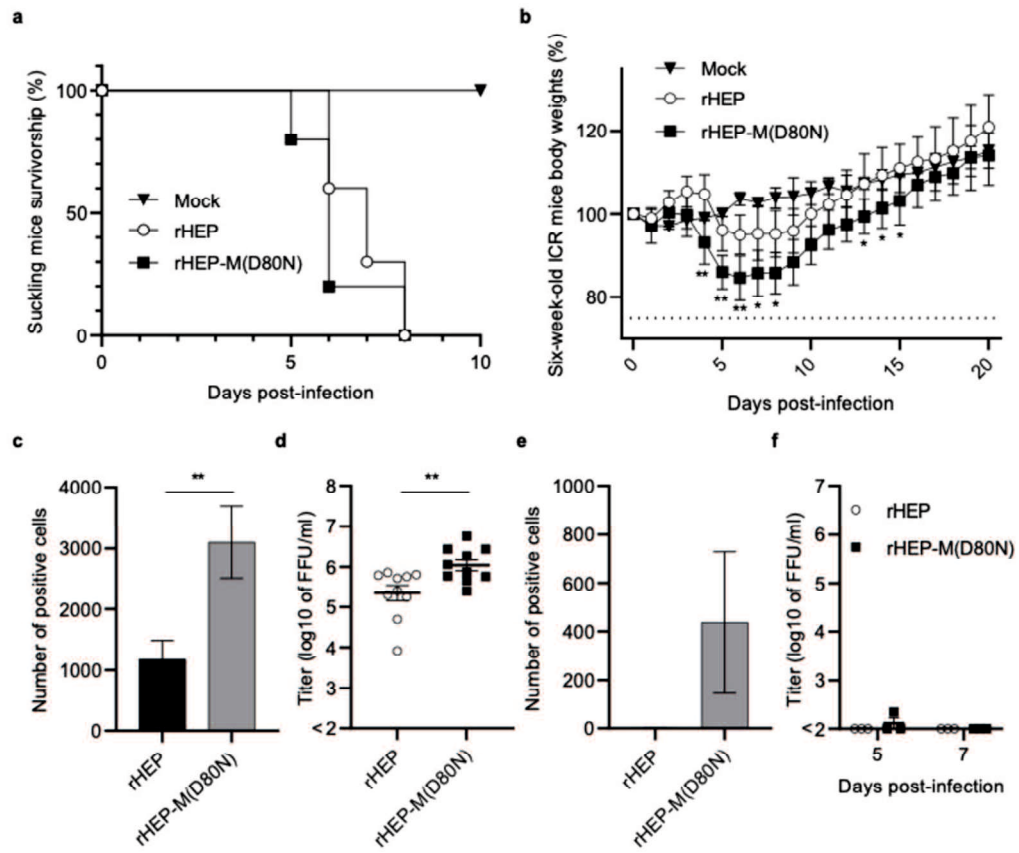
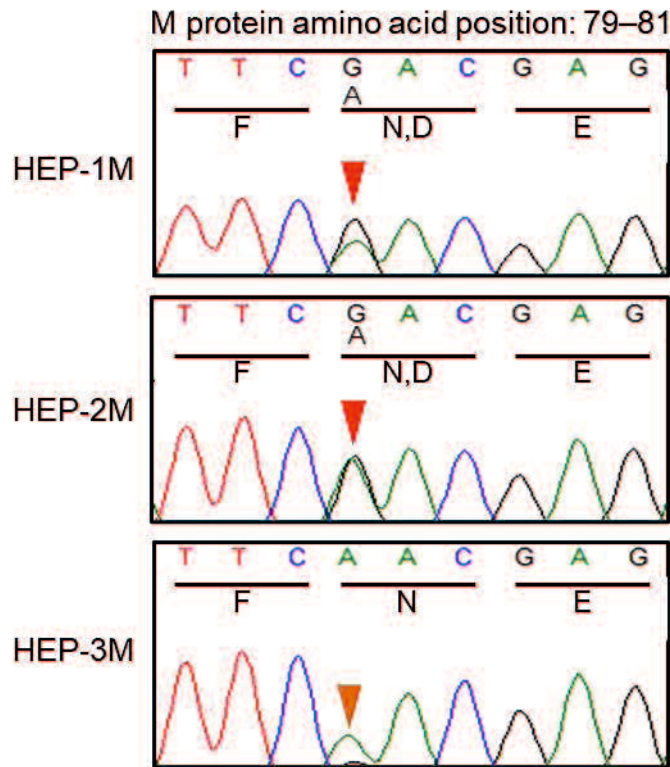


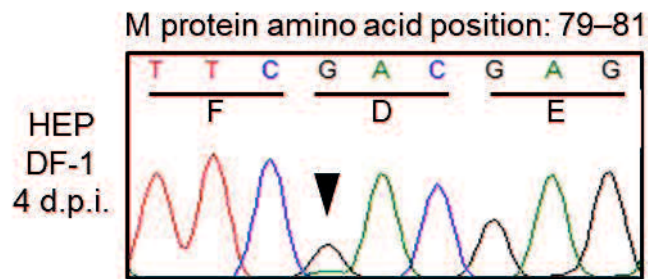
Fig. 2. Comparison of pathogenicity between rHEP and rHEP-M(D80N) in suckling and 6-week-old mice.

3.8 Supplemental figure and table



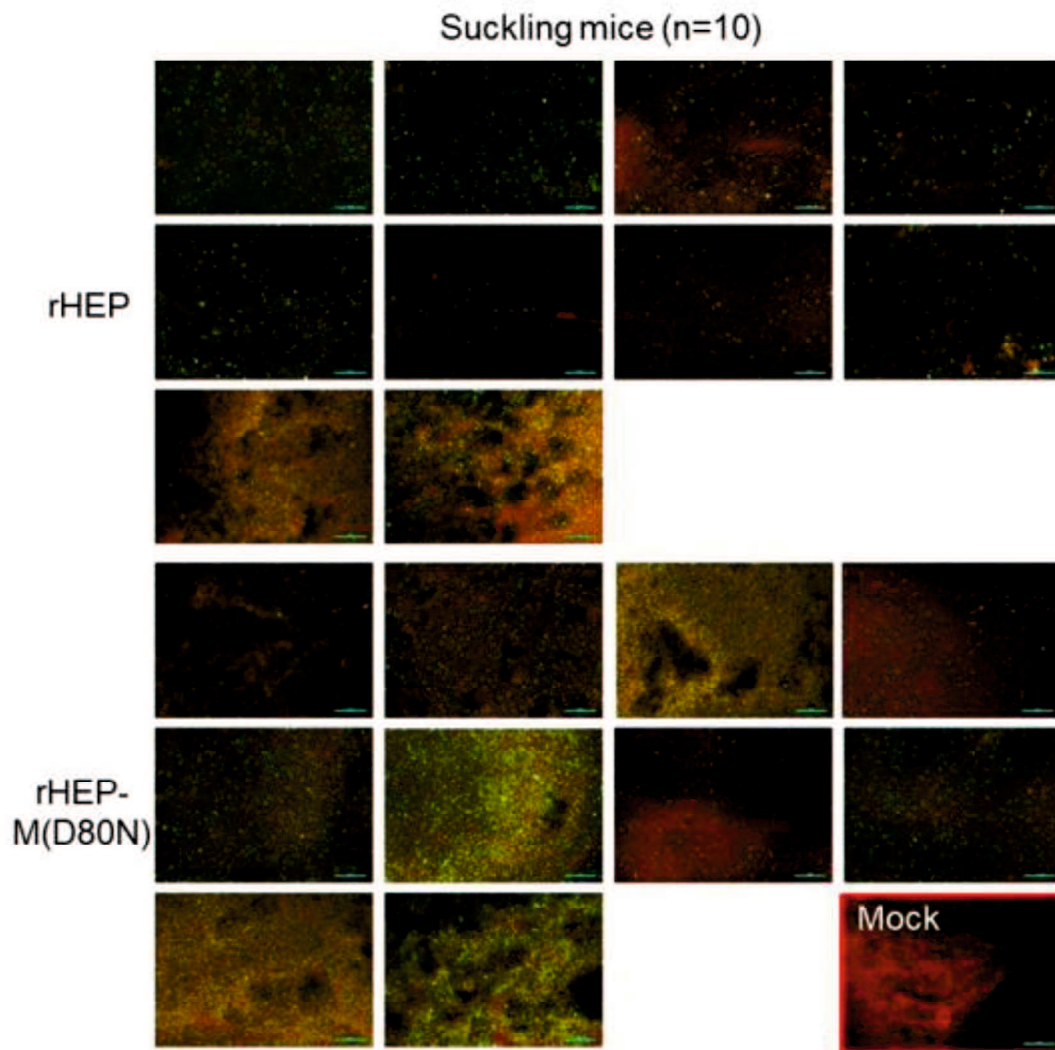
Supplemental Fig. S1 Comparison of nucleotide and amino acid sequences of original HEP-Flury after propagations in MNA cells.

The sequences of amino acids position 79 to 81 in the matrix (M) protein of propagated HEP strain after one, two, and three passages into MNA cells (HEP-1M, HEP-2M, and HEP-3M) are shown. Sequences of these strains were determined and compared using GENETYX Ver.15 (GENETYX, Tokyo, Japan) and a Sequence Scanner (Thermo Fisher Scientific, Waltham, MA, USA). At the nucleotide position of 238 (amino acid position 80) in the M protein, red arrowheads indicate a mixture of adenine and guanine, and the orange arrowhead indicates adenine.



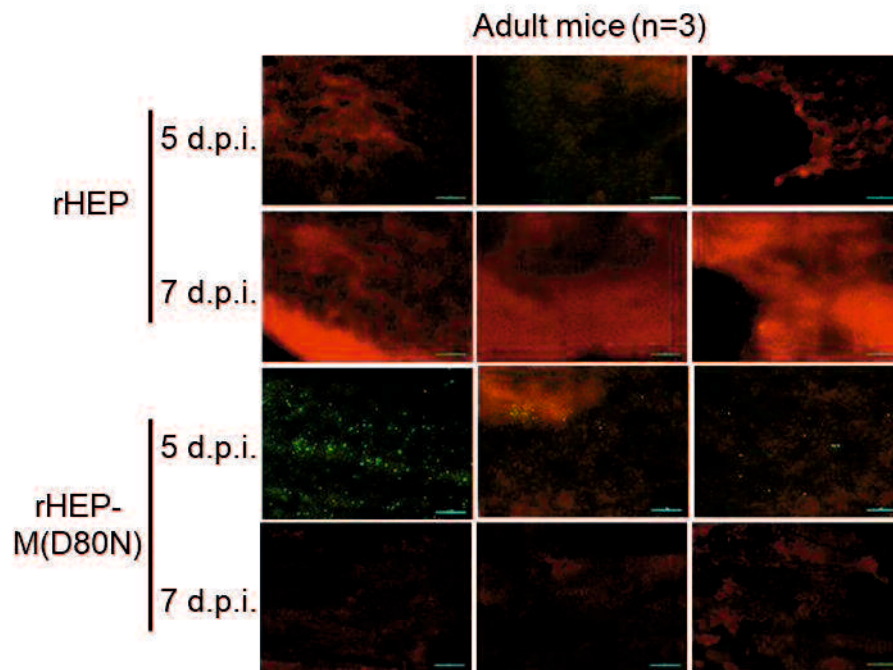
Supplemental Fig. S2 Nucleotide sequence of original HEP-Flury after propagation in chicken embryo fibroblast cells, DF-1.

The original HEP-Flury was inoculated to DF-1 cells at a multiplicity of infection (M.O.I.) of 0.05. The sequences were determined from the supernatant of DF-1 cells at 4 days post infection (d.p.i.) and compared using GENETYX Ver.15 (GENETYX, Tokyo, Japan) and a Sequence Scanner (Thermo Fisher Scientific, Waltham, MA, USA). The sequence at amino acid positions 79 to 81 in the matrix (M) protein are shown. Black arrowhead indicates guanine.



Supplemental Fig. S3 Direct fluorescent antibody test (DFAT) of brain samples of suckling mice inoculated with rHEP or rHEP-M(D80N).

Brain tissues were collected from suckling mice inoculated with either virus and applied to the slide with a toothpick. The slides were fixed in 10% formalin supplemented 0.4% Triton X-100 solution, stained with fluorescein isothiocyanate (FITC)-conjugated anti-rabies monoclonal globulin (FUJIREBIO, Tokyo, Japan), and examined under a fluorescence microscope. The stained samples were observed using NIS-Elements D version 5.20.00 imaging software (Nikon, Tokyo, Japan). RABV-positive cells appear green, while negative cells are stained red with Evans Blue. Scale bars, 100 μ m; magnification, $\times 40$. Brain samples from each of ten suckling mice that died at 5-8 d.p.i. after inoculation with either virus are shown.



Supplemental Fig. S4 Direct fluorescent antibody test (DFAT) of brain samples of adult mice inoculated with rHEP or rHEP-M(D80N).

Brain tissues were collected from adult mice inoculated with either virus and applied to the slide using a toothpick. The slides were fixed in 10% formalin supplemented 0.4% Triton X-100 solution, stained with FITC-conjugated anti-rabies monoclonal globulin, and examined under a fluorescence microscope. The stained samples were observed using NIS-Elements D version 5.20.00 imaging software. RABV-positive cells appear green, while negative cells are stained red with Evans Blue. Scale bars, 100 μm ; magnification, $\times 40$. Brain samples from adult mice inoculated with either virus are shown. Samples were collected from three mice at 5 and 7 d.p.i.

Supplemental Table S1 Primers used for PCR and construction of the full genome of the infectious clones.

Primer name	Orientation	Sequence (5'→3')	Position*
RABV 1	Forward	ACGCTTAACAACAAAACCAAAGAAG	1–25
	Reverse	TGAGCGATCTCAGCCTCYACTGATAG	2121–2096
RABV 2	Forward	CTCCGTTCACTAGGCTTGAGTGGG	934–958
	Reverse	GGACCAAGTTTGTCTGGTATCG	3412–3391
RABV 3	Forward	CTATGGTCTGACATGTCTCTTCAG	3033–3056
	Reverse	GACTTGGAATAGAAATGGGCCAAGTC	5790–5765
RABV 4	Forward	TGTCCCAACATCTTGAGGAACTC	5488–5511
	Reverse	CGCATTGGTGGATACTGTAGA	7912–7892
RABV 5	Forward	TACTAGCTCAAGGAGACAACCAGGT	7581–7605
	Reverse	AGCTGCATGGCGCACCTCTTGATC	10249–10226
RABV 6	Forward	CAGCTCAGGGGCTCTTATACTCAATC	9555–9580
	Reverse	ACGCTTAACAAATAAACAATAAAGAT	11925–11900
HEP-M_D80N	Forward	ATCATTCAACGAGATATACTCTGGGAA	2726–2752
	Reverse	ATCTCGTTGAATGATCTCAGAATATGC	2740–2714
Kpn_HamRz_HEP	Forward	<u>ATAGGTACCTGTTAAGCGTCTGATGAGTCCGTGAGGACGAAACTATAGGAAAGGAATTCCTA</u> <u>TAGTCACGCTTAACAACAAAACCAAAGAAGAAGCA</u> *	1–30
Pst_HdvRz_HEP	Reverse	<u>CGGCTGCAGCGCCCTCCCTTAGCCATCCGAGTGGACGTGCGTCCTCCTCGGATGCCAGG</u> <u>TCGGACCGCGAGGAGGTGGAGATGCCATGCCGACCCACGCTTAACAATAAACAATA</u> *	11925–11905

Ribozyme sequences are underlined.

* The positions of the primers for PCR and plasmid construction were defined according to the genomic sequence of the HEP strain.

Supplemental Table S2 Primers used to construct helper plasmids

Primer name	Orientation	Sequence (5'→3')	Position*
N protein	Forward	ATAGGTACCATGGATGCCGACAAG	67–85
	Reverse	CGGCTGCAGTTATGAGTCACTCG	1423–1410
P protein	Forward	ATAGGTACCATGAGCAAGATCTTTG	1511–1529
	Reverse	CGGCTGCAGTTAGCATGATGTGTAG	2408–2392
G protein	Forward	ATAGGTACCATGGTTCCTCAGGTTC	3318–3333
	Reverse	CGGCTGCAGTCACAGTCTGGTCTCG	4892–4877
L protein	Forward	ATAGGTACCATGCTGGATCCGGGA	5411–5425
	Reverse	CGGCTGCAGTTACAAACAAGTGTAG	11794–11779

* The positions of the primers for PCR and plasmid construction were defined according to the genomic sequence of the HEP strain.

4. General conclusion

Rabies is a fatal zoonotic encephalitis disease and the WHO promotes the “Zero by 30” plan to eliminate human rabies cases transmitted by dogs. One of the methods to prevent the rabies is vaccination. The vaccines are generated by passaging viruses in cell lines and animals. Therefore, understanding the mechanisms of adaptation is important for its application in the treatment and prevention of the disease.

In Chapter 1, we succeeded in generating Vero cell-adapted strains, HEP-10V and HEP-30V. In these strains, we found three and seven substitutions, respectively, that did not affect the pathogenicity but improved propagation in Vero cells. Five of these substitutions, P(L115H), G(S15R), G(V164E), G(L183P) and G(A286V), were important for adaptation of HEP-Flury in Vero cells. The recombinant RABV with these five substitutions, which we designated rHEP-PG4, is expected to serve as a candidate seed virus for propagation in Vero cells for vaccine production.

In Chapter 2, we found a single substitution in the M protein, M(D80N), by comparing between rHEP and HEP strains. This substitution did not affect growth in DF-1 cells but increased the propagation in MNA cells and mouse brain. As the result of the substitution, the pathogenicity was not changed from the parental strain except for the production of body weight loss. This novel finding demonstrates that the M protein is

associated with neurovirulence in mice and that the amino acid substitution M(D80N) may play a crucial role in this adaptation and neurovirulence.

Japan is one of the countries free from rabies, but Japan still possesses the risk of imported cases. Although, rabies vaccine contributes prevention of death from rabies in the world, further development of vaccine and treatment will be required to achieve “Zero by 30”. In Chapter 1, we generated a Vero cell-adapted vaccine strain that can reduce the cost and processing time of a vaccine production compared with conventional vaccine. In Chapter 2, we found M protein is associated with neurovirulence in mice.

These findings will help to improve the rabies vaccine by reduction the cost and processing time, and to develop the treatment targeting the M protein. Finally, it can contribute to the “Zero by 30” project to eliminate human rabies cases.

5. Acknowledgements

The present studies were conducted at the Department of Veterinary Science, National Institute of Infectious Disease from 2020 to 2024.

First of all, the author would like to express deep appreciation to her supervisor, **Dr. Ken Maeda** (Department of Veterinary Science, National Institute of Infectious Disease) for introduction of her to rabies research and for providing an environment where meaningful research can be conducted and also for his support in various tasks such as research design, experimentation, execution and investigation.

The author is also grateful to her co-supervisors, **Dr. Kyoko Tsukiyama-Kohara** (Transboundary Animal Disease Research Center, Kagoshima University) and **Dr. Hiroshi Shimoda** (Laboratory of Veterinary Microbiology, Yamaguchi University) for their advice and productive discussions on her studies.

The author is grateful as well to **Dr. Satoshi Inoue** and **Dr. Aya Matsuu** (Department of Veterinary Science, National Institute of Infectious Disease) for their advice, support, and suggestions on how to conduct the experiments in this report.

The author sincerely thanks the other members of the laboratory for their assistance in her research and for spending a very special time doing research with her.

Finally, the author would like to add a few words of appreciation to her family

members and husband for allowing and supporting her as a PhD student.

6. References

1. World Health Organization. *WHO Expert Consultation on Rabies: third report*. (World Health Organization, 2018).
2. Hampson, K., Coudeville, L., Lembo, T., *et al.* Estimating the global burden of endemic canine rabies. *PLoS Negl. Trop. Dis.* **9**, e0003709; 10.1371/journal.pntd.0003709 (2015).
3. Carrara, P., Parola, P., Brouqui, P., *et al.* Imported human rabies cases worldwide, 1990–2012. *PLoS Negl. Trop. Dis.* **7**, e2209; 10.1371/journal.pntd.0002209 (2013).
4. Nosaki, Y., Maeda, K., Watanabe, M., *et al.* Fourth imported rabies case since the eradication of rabies in Japan in 1957. *J. Travel Med.* **28**, taab151; 10.1093/jtm/taab151 (2021).
5. World Health Organization, Food and Agriculture Organization of the United Nations, & World Organisation for Animal Health. *Zero by 30: the global strategic plan to end human deaths from dog-mediated rabies by 2030*. (World Health Organization, 2018).
6. Wu, X., Smith, T. G. & Rupprecht, C. E. From brain passage to cell adaptation: the road of human rabies vaccine development. *Expert Rev. Vaccines* **10**, 1597–1608; 10.1586/erv.11.140 (2011).
7. World Health Organization, Food and Agriculture Organization of the United Nations,

- & World Organisation for Animal Health. *Zero by 30: the global strategic plan to end human deaths from dog-mediated rabies by 2030: United Against Rabies Collaboration: first annual progress report: global strategic plan to end human deaths from dog-mediated rabies by 2030*. (World Health Organization, 2019).
8. Fooks, A. R., Cliquet, F., Finke, S., *et al.* Rabies. *Nat. Rev. Dis. Primer* **3**, 17091; 10.1038/nrdp.2017.91 (2017).
 9. Albertini, A. A. V., Ruigrok, R. W. H. & Blondel, D. Rabies virus transcription and replication. *Advances in Virus Research* vol. 79 1–22 (Academic Press, 2011).
 10. Schnell, M. J., McGettigan, J. P., Wirblich, C., *et al.* The cell biology of rabies virus: using stealth to reach the brain. *Nat. Rev. Microbiol.* **8**, 51–61; 10.1038/nrmicro2260 (2010).
 11. Lafon, M. Rabies virus receptors. *J. Neurovirol.* **11**, 82–87; 10.1080/13550280590900427 (2005).
 12. Rieder, M. & Conzelmann, K.-K. Interferon in rabies virus infection. *Advances in Virus Research* vol. 79 91–114 (Academic Press, 2011).
 13. Yin, J., Wang, X., Mao, R., *et al.* Research advances on the interactions between rabies virus structural proteins and host target cells: accrued knowledge from the application of reverse genetics systems. *Viruses* **13**, 2288; 10.3390/v13112288 (2021).

14. Ito, N., Moseley, G. W. & Sugiyama, M. The importance of immune evasion in the pathogenesis of rabies virus. *J. Vet. Med. Sci.* **78**, 1089–1098; 10.1292/jvms.16-0092 (2016).
15. Baer, G. M. *The natural history of rabies.* (Routledge, 2017). doi:10.1201/9780203736371.
16. Boland, T. A., McGuone, D., Jindal, J., *et al.* Phylogenetic and epidemiologic evidence of multiyear incubation in human rabies. *Ann. Neurol.* **75**, 155–160; 10.1002/ana.24016 (2014).
17. Aramburo, A., Willoughby, R. E., Bollen, A. W., *et al.* Failure of the Milwaukee protocol in a child with rabies. *Clin. Infect. Dis.* **53**, 572–574; 10.1093/cid/cir483 (2011).
18. Kumar, S. K., Gupta, P. & Panda, P. K. Death from rabies: the reason being poor compliance to vaccination or it's failure. *J. Fam. Med. Prim. Care* **9**, 4437–4440; 10.4103/jfmpe.jfmpe_658_20 (2020).
19. Tolentino Júnior, D. S., Marques, M. S. V., Krummenauer, A., *et al.* Rabies outbreak in Brazil: first case series in children from an indigenous village. *Infect. Dis. Poverty* **12**, 78; 10.1186/s40249-023-01130-y (2023).
20. Rappuoli, R. 1885, the first rabies vaccination in humans. *Proc. Natl. Acad. Sci.* **111**,

- 12273–12273; 10.1073/pnas.1414226111 (2014).
21. Sellers, T. F. Rabies, the physician's dilemma. *Am. J. Trop. Med. Hyg.* **s1-28**, 453–456; 10.4269/ajtmh.1948.s1-28.453 (1948).
22. Bonito, R. F., Oliveira, N. M. de & Nishioka, S. de A. Adverse reactions associated with a Fuenzalida-Palacios rabies vaccine: a quasi-experimental study. *Rev. Soc. Bras. Med. Trop.* **37**, 7–9; 10.1590/S0037-86822004000100002 (2004).
23. Goodpasture, E. W., Woodruff, A. M. & Buddingh, G. J. The cultivation of vaccine and other viruses in the chorio-allantoic membrane of chick embryos. *Science* **74**, 371–372; 10.1126/science.74.1919.371 (1931).
24. Leach, C. N. & Johnson, H. N. Human rabies, with special reference to virus distribution and titer. *Am. J. Trop. Med. Hyg.* **s1-20**, 335–340; 10.4269/ajtmh.1940.s1-20.335 (1940).
25. Horiya, M., Posadas-Herrera, G., Takayama-Ito, M., *et al.* Genetic characterization of human rabies vaccine strain in Japan and rabies viruses related to vaccine development from 1940s to 1980s. *Viruses* **14**; 10.3390/v14102152 (2022).
26. Takayama-Ito, M., Inoue, K., Shoji, Y., *et al.* A highly attenuated rabies virus HEP-Flury strain reverts to virulent by single amino acid substitution to arginine at position 333 in glycoprotein. *Virus Res.* **119**, 208–215; 10.1016/j.virusres.2006.01.014 (2006).

27. Preiss, S., Chanthavanich, P., Chen, L. H., *et al.* Post-exposure prophylaxis (PEP) for rabies with purified chick embryo cell vaccine: a systematic literature review and meta-analysis. *Expert Rev. Vaccines* **17**, 525–545; 10.1080/14760584.2018.1473765 (2018).
28. Tao, L., Ge, J., Wang, X., *et al.* Molecular basis of neurovirulence of Flury rabies virus vaccine strains: importance of the polymerase and the glycoprotein R333Q mutation. *J. Virol.* **84**, 8926–8936; 10.1128/JVI.00787-10 (2010).
29. Itakura, Y., Tabata, K., Morimoto, K., *et al.* Glu333 in rabies virus glycoprotein is involved in virus attenuation through astrocyte infection and interferon responses. *iScience* **25**, 104122; 10.1016/j.isci.2022.104122 (2022).
30. Wang, S.-Y., Sun, J.-F., Liu, P., *et al.* Immunogenicity and safety of human diploid cell vaccine (HDCV) vs. purified Vero cell vaccine (PVRV) vs. purified chick embryo cell vaccine (PCECV) used in post-exposure prophylaxis: a systematic review and meta-analysis. *Hum. Vaccines Immunother.* **18**, 2027714; 10.1080/21645515.2022.2027714 (2022).
31. Banyard, A. C., McElhinney, L. M., Johnson, N., *et al.* Introduction history of rabies control by vaccination. *Rev. Sci. Tech.* **37**, 305–322; 10.20506/rst.37.2.2804 (2018).
32. World Health Organization. *Rabies: rationale for investing in the global elimination*

- of dog-mediated human rabies.* (World Health Organization, 2015).
33. Kuhn, J. H., Adkins, S., Agwanda, B. R., *et al.* 2021 taxonomic update of phylum Negarnaviricota (Riboviria: Orthornavirae), including the large orders Bunyavirales and Mononegavirales. *Arch. Virol.* **166**, 3513–3566; 10.1007/s00705-021-05143-6 (2021).
34. Finke, S. & Conzelmann, K.-K. Replication strategies of rabies virus. *Virus Res.* **111**, 120–131; 10.1016/j.virusres.2005.04.004 (2005).
35. Fooks, A. R., Banyard, A. C., Horton, D. L., *et al.* Current status of rabies and prospects for elimination. *The Lancet* **384**, 1389–1399; 10.1016/S0140-6736(13)62707-5 (2014).
36. Evans, J. S., Selden, D., Wu, G., *et al.* Antigenic site changes in the rabies virus glycoprotein dictates functionality and neutralizing capability against divergent lyssaviruses. *J. Gen. Virol.* **99**, 169–180; 10.1099/jgv.0.000998 (2018).
37. Ashwathnarayana, D. H., Madhusudana, S. N., Sampath, G., *et al.* A comparative study on the safety and immunogenicity of purified duck embryo cell vaccine (PDEV, Vaxirab) with purified chick embryo cell vaccine (PCEC, Rabipur) and purified vero cell rabies vaccine (PVRV, Verorab). *Vaccine* **28**, 148–151; 10.1016/j.vaccine.2009.09.090 (2009).

38. Ammerman, N. C., Beier-Sexton, M. & Azad, A. F. Growth and maintenance of Vero cell lines. *Curr. Protoc. Microbiol.* **APPENDIX**, Appendix-4E; 10.1002/9780471729259.mca04es11 (2008).
39. Montagnon, B. J. Inactivated polio vaccine: industrial production from micro-carrier Vero cells culture. *Trop. Geogr. Med.* **37**, S40-41 (1985).
40. World Health Organization. Polio vaccines: WHO position paper – June 2022. *Wkly. Epidemiol. Rec.* **25**, 277–300 (2022).
41. Suntharasamai, P., Chanthavanich, P., Warrell, M. J., *et al.* Purified Vero cell rabies vaccine and human diploid cell strain vaccine: comparison of neutralizing antibody responses to post-exposure regimens. *J. Hyg. (Lond.)* **96**, 483–489 (1986).
42. Pasteur, M. Infectious diseases and vaccination for rabies. *Atlanta Med. Surg. J.* **1884**, 1, 437–448 (1884).
43. Lafon, M., Bourhy, H. & Sureau, P. Immunity against the European bat rabies (Duvénhage) virus induced by rabies vaccines: an experimental study in mice. *Vaccine* **6**, 362–368; 10.1016/0264-410X(88)90184-3 (1988).
44. Moulenat, T., Petit, C., Bosch Castells, V., *et al.* Purified Vero cell rabies vaccine (PVRV, Verorab®): a systematic review of intradermal use between 1985 and 2019. *Trop. Med. Infect. Dis.* **5**, 40; 10.3390/tropicalmed5010040 (2020).

45. Hashimoto, M. & Yoshino, K. Alteration of the *in vitro* host range of rabies virus after serial chick embryo cell passage using alkaline maintenance medium. *Jpn. J. Microbiol.* **20**, 339–346; 10.1111/j.1348-0421.1976.tb00996.x (1976).
46. V, K. Biphasic demyelination of the nervous system following anti-rabies vaccination. *Neurol. India* **52**, 106 (2004).
47. World Health Organization. Measuring effectiveness and impact of Japanese encephalitis vaccination. *World Health Organ.* (2016).
48. World Health Organization. Japanese encephalitis vaccines: WHO position paper, February 2015 – Recommendations. *Vaccine* **34**, 302–303; 10.1016/j.vaccine.2015.07.057 (2016).
49. Ito, N., Takayama, M., Yamada, K., *et al.* Rescue of rabies virus from cloned cDNA and identification of the pathogenicity-related gene: glycoprotein gene is associated with virulence for adult mice. *J. Virol.* **75**, 9121–9128; 10.1128/JVI.75.19.9121-9128.2001 (2001).
50. World Health Organization, Rupprecht, C. E., Fooks, A. R., *et al.* *Laboratory techniques in rabies, volume 1.* (World Health Organization, 2018).
51. Smith, J. S., Yager, P. A. & Baer, G. M. A rapid reproducible test for determining rabies neutralizing antibody. *Bull. World Health Organ.* **48**, 535–541 (1973).

52. World Health Organization, Rupprecht, C. E., Fooks, A. R., *et al.* *Laboratory techniques in rabies, volume 2.* (World Health Organization, 2019).
53. Hamamoto, N., Uda, A., Tobiume, M., *et al.* Association between RABV G proteins transported from the perinuclear space to the cell surface membrane and N-glycosylation of the sequon Asn(204). *Jpn. J. Infect. Dis.* **68**, 387–393; 10.7883/yoken.JJID.2014.533 (2015).
54. Inoue, K., Shoji, Y., Kurane, I., *et al.* An improved method for recovering rabies virus from cloned cDNA. *J. Virol. Methods* **107**, 229–236; 10.1016/S0166-0934(02)00249-5 (2003).
55. Kaku, Y., Noguchi, A., Marsh, G. A., *et al.* Second generation of pseudotype-based serum neutralization assay for Nipah virus antibodies: Sensitive and high-throughput analysis utilizing secreted alkaline phosphatase. *J. Virol. Methods* **179**, 226–232; 10.1016/j.jviromet.2011.11.003 (2012).
56. Fouquet, B., Nikolic, J., Larrous, F., *et al.* Focal adhesion kinase is involved in rabies virus infection through its interaction with viral phosphoprotein P. *J. Virol.* **89**, 1640–1651; 10.1128/JVI.02602-14 (2015).
57. Ilic, D., Damsky, C. H. & Yamamoto, T. Focal adhesion kinase: at the crossroads of signal transduction. *J. Cell Sci.* **110**, 401–407; 10.1242/jcs.110.4.401 (1997).

58. Parsons, J. T. Focal adhesion kinase: the first ten years. *J. Cell Sci.* **116**, 1409–1416; 10.1242/jcs.00373 (2003).
59. Takayama-Ito, M., Ito, N., Yamada, K., *et al.* Multiple amino acids in the glycoprotein of rabies virus are responsible for pathogenicity in adult mice. *Virus Res.* **115**, 169–175; 10.1016/j.virusres.2005.08.004 (2006).
60. Yamada, K., Noguchi, K. & Nishizono, A. Efficient N-glycosylation at position 37, but not at position 146, in the street rabies virus glycoprotein reduces pathogenicity. *Virus Res.* **179**, 169–176; 10.1016/j.virusres.2013.10.015 (2014).
61. Faber, M., Faber, M.-L., Papaneri, A., *et al.* A single amino acid change in rabies virus glycoprotein increases virus spread and enhances virus pathogenicity. *J. Virol.* **79**, 14141–14148; 10.1128/jvi.79.22.14141-14148.2005 (2005).
62. Irie, T., Matsuda, Y., Honda, Y., *et al.* Studies on the escape mutants of rabies virus which are resistant to neutralization by a highly conserved conformational epitope-specific monoclonal antibody #1-46-12. *Microbiol. Immunol.* **46**, 449–461; 10.1111/j.1348-0421.2002.tb02719.x (2002).
63. Nagarajan, T., Marissen, W. & Rupprecht, C. Monoclonal antibodies for the prevention of rabies: theory and clinical practice. *Antib. Technol. J.* **1**; 10.2147/ANTI.S33533 (2014). doi:10.2147/ANTI.S33533.

64. Yamada, K., Park, C.-H., Noguchi, K., *et al.* Serial passage of a street rabies virus in mouse neuroblastoma cells resulted in attenuation: Potential role of the additional N-glycosylation of a viral glycoprotein in the reduced pathogenicity of street rabies virus. *Virus Res.* **165**, 34–45; 10.1016/j.virusres.2012.01.002 (2012).
65. Langevin, C. & Tuffereau, C. Mutations conferring resistance to neutralization by a soluble form of the neurotrophin receptor (p75NTR) map outside of the known antigenic sites of the rabies virus glycoprotein. *J. Virol.* **76**, 10756–10765; 10.1128/jvi.76.21.10756-10765.2002 (2002).
66. Sasaki, M., Anindita, P. D., Ito, N., *et al.* The role of heparan sulfate proteoglycans as an attachment factor for rabies virus entry and infection. *J. Infect. Dis.* **217**, 1740–1749; 10.1093/infdis/jiy081 (2018).
67. Lentz, T. L., Burrage, T. G., Smith, A. L., *et al.* Is the acetylcholine receptor a rabies virus receptor? *Science* **215**, 182–184; 10.1126/science.7053569 (1982).
68. Thoulouze, M.-I., Lafage, M., Schachner, M., *et al.* The neural cell adhesion molecule is a receptor for rabies virus. *J. Virol.* **72**, 7181–7190; 10.1128/JVI.72.9.7181-7190.1998 (1998).
69. Tuffereau, C., Bénéjean, J., Blondel, D., *et al.* Low-affinity nerve-growth factor receptor (P75NTR) can serve as a receptor for rabies virus. *EMBO J.* **17**, 7250–7259;

- 10.1093/emboj/17.24.7250 (1998).
70. Wang, J., Wang, Z., Liu, R., *et al.* Metabotropic glutamate receptor subtype 2 is a cellular receptor for rabies virus. *PLOS Pathog.* **14**, e1007189; 10.1371/journal.ppat.1007189 (2018).
71. Andersen, J. H., Jenssen, H., Sandvik, K., *et al.* Anti-HSV activity of lactoferrin and lactoferricin is dependent on the presence of heparan sulphate at the cell surface. *J. Med. Virol.* **74**, 262–271; 10.1002/jmv.20171 (2004).
72. Molecular Operating Environment (MOE), 2022.02 chemical computing group ULC, 910-1010 Sherbrooke St. W., Montreal, QC H3A 2R7, Canada. (2023).
73. Song, Y., Li, L., Ma, T., *et al.* A novel mouse model for polysynaptic retrograde tracing and rabies pathological research. *Cell. Mol. Neurobiol.* **43**, 3743–3752; 10.1007/s10571-023-01384-y (2023).
74. Scott, T. P. & Nel, L. H. Lyssaviruses and the fatal encephalitic disease rabies. *Front. Immunol.* **12**, (2021).
75. Shimazaki, Y., Inoue, S., Takahashi, C., *et al.* Immune response to Japanese rabies vaccine in domestic dogs. *J. Vet. Med. Ser. B* **50**, 95–98; 10.1046/j.1439-0450.2003.00627.x (2003).
76. Fallahi, F., Wandeler, A. I. & Nadin-Davis, S. A. Characterization of epitopes on the

- rabies virus glycoprotein by selection and analysis of escape mutants. *Virus Res.* **220**, 161–171; 10.1016/j.virusres.2016.04.019 (2016).
77. Park, J.-S., Um, J., Choi, Y.-K., *et al.* Immunostained plaque assay for detection and titration of rabies virus infectivity. *J. Virol. Methods* **228**, 21–25; 10.1016/j.jviromet.2015.10.010 (2016).
78. Liu, X., Yang, Y., Sun, Z., *et al.* A recombinant rabies virus encoding two copies of the glycoprotein gene confers protection in dogs against a virulent challenge. *PLoS ONE* **9**, e87105; 10.1371/journal.pone.0087105 (2014).
79. Astawa, I. N. M., Agustini, N. L. P., Masa Tenaya, I. W., *et al.* Protective antibody response of Balb/c mice to Bali rabies virus isolate propagated in BHK-21 cells. *J. Vet. Med. Sci.* **80**, 1596–1603; 10.1292/jvms.17-0385 (2018).
80. Liu, Y., Zhang, S., Zhang, F., *et al.* Adaptation of a Chinese ferret badger strain of rabies virus to high-titered growth in BHK-21 cells for canine vaccine development. *Arch. Virol.* **157**, 2397–2403; 10.1007/s00705-012-1436-2 (2012).
81. Li, C., Wang, Y., Liu, H., *et al.* Change in the single amino acid Site 83 in rabies virus glycoprotein enhances the BBB permeability and reduces viral pathogenicity. *Front. Cell Dev. Biol.* **8**, 632957; 10.3389/fcell.2020.632957 (2021).
82. Mita, T., Shimizu, K., Ito, N., *et al.* Amino acid at position 95 of the matrix protein is

- a cytopathic determinant of rabies virus. *Virus Res.* **137**, 33–39; 10.1016/j.virusres.2008.05.011 (2008).
83. Finke, S., Granzow, H., Hurst, J., *et al.* Intergenotypic replacement of lyssavirus matrix proteins demonstrates the role of lyssavirus M proteins in intracellular virus accumulation. *J. Virol.* **84**, 1816–1827; 10.1128/jvi.01665-09 (2010).
84. Finke, S. & Conzelmann, K.-K. Dissociation of rabies virus matrix protein functions in regulation of viral RNA synthesis and virus assembly. *J. Virol.* **77**, 12074–12082; 10.1128/jvi.77.22.12074-12082.2003 (2003).
85. Harty, R. N., Paragas, J., Sudol, M., *et al.* A proline-rich motif within the matrix protein of vesicular stomatitis virus and rabies virus interacts with WW domains of cellular proteins: implications for viral budding. *J. Virol.* **73**, 2921–2929; 10.1128/jvi.73.4.2921-2929.1999 (1999).
86. Wirblich, C., Tan, G. S., Papaneri, A., *et al.* PPEY motif within the rabies virus (RV) matrix protein is essential for efficient virion release and RV pathogenicity. *J. Virol.* **82**, 9730–9738; 10.1128/JVI.00889-08 (2008).
87. Zhang, W., Liu, Y., Li, M., *et al.* Host desmin interacts with RABV matrix protein and facilitates virus propagation. *Viruses* **15**, 434; 10.3390/v15020434 (2023).
88. Kojima, I., Izumi, F., Ozawa, M., *et al.* Analyses of cell death mechanisms related to

- amino acid substitution at position 95 in the rabies virus matrix protein. *J. Gen. Virol.* **102**, 001594; 10.1099/jgv.0.001594 (2021).
89. Sonthonnax, F., Besson, B., Bonnaud, E., *et al.* Lyssavirus matrix protein cooperates with phosphoprotein to modulate the Jak-Stat pathway. *Sci. Rep.* **9**, 12171; 10.1038/s41598-019-48507-4 (2019).
90. Feige, L., Kozaki, T., Dias de Melo, G., *et al.* Susceptibilities of CNS cells towards rabies virus infection is linked to cellular innate immune responses. *Viruses* **15**, 88; 10.3390/v15010088 (2023).
91. Pulmanusahakul, R., Li, J., Schnell, M. J., *et al.* The glycoprotein and the matrix protein of rabies virus affect pathogenicity by regulating viral replication and facilitating cell-to-cell spread. *J. Virol.* **82**, 2330–2338; 10.1128/JVI.02327-07 (2008).